Socio-ecological Systems Model to Study Indian Oil Sardine Fisheries Dynamics in Kerala

A Thesis

submitted to

Indian Institute of Science Education and Research Pune

in partial fulfillment of the requirements for the

BS-MS Dual Degree Programme

by

Adish Assain Illikkal

Indian Institute of Science Education and Research Pune

Dr. Homi Bhabha Road,

Pashan, Pune 411008, INDIA.

May, 2023

Supervisors: Dr Amit Apte, Dr Steven Lade

Certificate

This is to certify that this dissertation entitled " Socio-ecological Systems Model to Study Indian Oil Sardine Fisheries Dynamics in Kerala " towards the partial fulfilment of the BS-MS dual degree programme at the Indian Institute of Science Education and Research, Pune represents study/work carried out by Adish Assain Illikkal at Indian Institute of Science Education and Research, Pune under the supervision of Dr Amit Apte, Professor and Chair, Data Science, Indian Institute of Science Education and Research, Pune and Dr Steven Lade, ARC Future Fellow at Fenner School of Environment and Society, ANU College of Science , Australia, during the academic year 2022-2023.

Dr Amit Apte   Dr Steven Lade

Committee:

Dr Amit Apte

Dr Steven Lade

*" There are so many things we can do if we focus on antiknowledge,
or what we do not know."*

— **Nassim Nicholas Taleb**

Declaration

I hereby declare that the matter embodied in the report entitled Socio-ecological Systems Model to Study Indian Oil Sardine Fisheries Dynamics in Kerala   are the results of the work carried out by me at the Data Science, Indian Institute of Science Education and Research, Pune, Indian Institute of Science Education and Research, Pune, under the supervision of Dr Amit Apte and Dr Steven Lade, and the same has not been submitted elsewhere for any other degree.

Adish Assain Illikkal

Acknowledgments

have been invaluable to me. I am grateful for their sacrifices and for instilling in me the values of dedication, perseverance, and compassion. Without them, I would not be where I am today, and for that, I am forever indebted to them.

Abstract

The collapse of the Indian Oil Sardine (IOS) fishery in the early 2010s has had devastating effects on the livelihoods of thousands of small-scale fisherfolk in Kerala. Previous studies have analyzed the decline of IOS fish populations using conventional fisheries models that often oversimplify complex interactions and assume linear relationships, neglecting the nonlinearity and feedback loops that can be critical in understanding the dynamics of ecological systems. In contrast, our study employs a dynamical systems model to investigate the regime shift of IOS fisheries by capturing the complex interplay of ecological and social processes involved in the system. Our results demonstrate that the stability of the sardine fisheries system can be attributed to both fisher behaviour and environmental factors (upwelling, migration), and highlight the importance of addressing both factors for sustainable management of the fishery.

Contents

List of Figures

List of Tables

List of Abbreviations

CPUE	Catch Per Unit Effort	JFS	Jellyfish Senescence
DOR	Degree of Regulation	LFT	Loss in Fishing Time
FG	Fishing Gear	MN	Migration Number
FGIBRS	Fishing Gear (Inboard Ring Seine)	PHY	Phytoplankton Density
FGOBRS	Fishing Gear (Outboard Ring Seine)	PPCJ	Phytoplankton Consumption Juvenile
FCT	Fishing Compensated Time	SC	Sardine Catch
FT	Fishing Time	FG	Fishing Gear
GE	Gear Exit	SMN	Sardine Mortality Natural
JFG	Jellyfish Growth	SJN	Sardine Juvenile Number
JFN	Jellyfish Number	SN	Sardine Number
JFMS	Jellyfish Medusa Strobilation	SRIA	Sardine Recruitment Into Adult
JFPM	Jellyfish Predation Mortality		

Chapter 1

Introduction

Background

Indian Oil Sardine, *Sardinella longiceps,* is an economically important small pelagic fish species found in tropical waters of the southeastern Arabian Sea. Fish is commonly used in various traditional dishes in Kerala and is an important source of protein and nutrition for local communities. However, in the last decade, the abundance of sardine fish population has drastically declined due to deteriorating environmental conditions and overfishing (Kripa et al., 2018). The stock of this resource is vulnerable to significant annual fluctuations due to various anthropogenic (e.g., overfishing), biological (e.g. spawning failure, competition from other species occupying the same niche, and food shortages), and environmental (e.g. El Niño, rising sea surface temperatures, erratic rainfall, and other climatic events) factors. These factors are believed to have a significant impact on the landings of this resource (Rohit et al., 2018).

In 2012, this resource achieved a record-breaking level of landings, yet within three years, the fishery collapsed. Several studies have been conducted to comprehend the underlying causes of this sudden collapse, and numerous policy recommendations have been proposed based on the findings of fisheries researchers (Kripa et al., 2018; Mohamed et al., 2014). The government introduced management tools like minimum legal size (MLS) with the ability to protect juvenile fish, maintain spawning stocks and control the sizes of fish caught.

Research gap

Although researchers have identified several potential factors that might have led to the collapse of the system, we do not know the extent of the interactions between these factors and how they may have contributed to the collapse of the Indian oil sardine fishery. We were particularly interested in understanding the complex interplay of social and ecological processes that characterize the dynamics of IOS fisheries.

The dynamics of social-ecological systems arise due to interconnected feedback loops among biophysical processes, human behaviours, and institutional processes within specific social and biophysical contexts (Reyers et al., 2018). Understanding the dynamical interplay between the constituents of systems is challenging. Conventional dynamical models of complex systems are rarely mathematically tractable, and their numerical exploration suffers both from computational and data limitations (Massing and Gross, 2021). Here, we use a generalized modeling approach (Gross and Feudel, 2006) that can deal with limited data availability by relying on causal relationships drawn from cross-disciplinary knowledge from academic and grey literature, including research articles, newsletters, policy reports, and annual reports. We use concepts such as stability to distinguish between qualitatively different features of the system.

Research approach and methodology

We will adopt a research approach that employs dynamical systems modeling to study the intricate causal interactions and behaviours of fisheries as a complex system. Conventional models often involve a set of differential equations that precisely define the time evolution of each variable. Generalized modeling in dynamical systems acknowledges the limitations of empirical knowledge and does not assume a single definitive truth. Instead, it considers a range of possibilities that are consistent with the available structural knowledge. By exploring the dynamics within this ensemble, researchers can gain a better understanding of the potential outcomes and narrow down the set of possible models. This approach provides a more comprehensive understanding of dynamical systems while acknowledging the uncertainties inherent in such models. Generalized modeling enables researchers to create flexible frameworks for further exploration and refinement of the model, making it a

valuable tool for empirical modeling in the face of uncertainty.

Generalized modeling approach has been utilized several times previously and has been adapted to suit various fields. Initial studies focused on prey-predator models and food web models (Gross, 2004; Gross et al., 2005). The tractability of Jacobian matrices through generalized ecological models led to their use as a foundation for various methodological advancements. The approach was improved by (Yeakel et al., 2011), and (Kuehn et al., 2013) extended the approach with rigorous mathematical support. (Lade and Gross, 2012) proposed a new type of warning signal for critical transitions based on Generalized modeling. The approach was subsequently applied to examine empirical socio-ecological systems, emphasizing the importance of system stability (Lade and Niiranen, 2017).

Stability in dynamical systems refers to the tendency of a system to return to its initial state or to remain in a certain state after a small perturbation. In a dynamical system, a stable fixed point (Holmes and Shea-Brown, 2006) is an equilibrium point around which the system remains within a basin of attraction (Ott, 2006), and any small perturbation of the system's state causes it to converge back to the fixed point over time. The eigenvalues of a matrix that describes the linearization of the system at an equilibrium point determine the stability of that equilibrium. Specifically, if all the eigenvalues have negative real parts, the equilibrium is said to be asymptotically stable, meaning that the system will converge to the equilibrium point over time. In this work, we use the real part of the dominant eigenvalue of the jacobian matrix of the system of differential equations to represent instability. However, this can be misleading in systems like large networks as instabilities can often arise on very different timescales, such that the eigenvalue that is the leading one in most of the parameter space may not be the one that causes the instability once stability is lost (Massing and Gross, 2021).

Generalized models also permit analyses of the stability of other attractors like limit cycles (Kuehn et al., 2013). However, in the case of sardine fisheries, a fixed point is assumed even though the system need not reside exactly at the fixed point. The system may oscillate within the basin of attraction around the fixed point. The fixed point may also shift slowly in time due to the effects of slow variables (Kuehn, 2011). In order to simplify the investigation of the regime shift in the fisheries system, we limited our analysis to the local dynamics of the system near the equilibria.

Significance of study

In fisheries, regime shift can occur when a fishery system experiences a significant and often abrupt change in its productivity, composition, or structure, leading to a new state that is different from the previous state (such as fisheries collapse characterized by a low abundance regime). The present study aims to understand the role of different components (variables, drivers) in the regime shift of the fisheries system and test different assumptions using a formal modeling framework. Building upon existing work, we provide a more rigorous and generalized derivation of the methodology for systems with arbitrary numbers of state variables and intermediate variables, resulting in a clearer and more comprehensive understanding of the underlying framework and its practical applications. Our findings reveal that the stability of the sardine fisheries system is influenced by a combination of fisher behaviour and environmental factors, such as upwelling and migration. Moreover, we demonstrate that the presence of uncertainty in non-linear links (elasticities) plays a key role in understanding regime shifts.

Scope and limitations

Dynamical systems modeling provides an effective means to explore the behaviour of complex systems, particularly in data-scarce environments. It enables the exploration of interesting parameter regions and phenomena based on limited information, thus speeding up the initial exploration. As we gain new insights and data, we may need to update the model to reflect these changes. However, these models may not be suitable for representing individual actors' roles and decision-making processes. Although model builders can include actor heterogeneity and decision-making processes through causal relationships, these representations may be less intuitive than those in agent-based modeling. Moreover, Andrei Saltelli has identified several limitations of dynamical systems modeling, including the reliance on unverified assumptions, the compression and linearization of analysis to convey an impression of control and prediction, and the absence of sensitivity analysis (Saltelli and Giampietro, 2015). Despite these limitations, dynamical systems modeling offers the advantage of iteratively expanding generalized models to incorporate new insights into the system, enabling sensitivity analysis and the potential for iterative model improvement

Chapter 2

Materials and Methods

2.1 Data

The data required for the estimation of generalized parameters were obtained from pre-existing literature based on empirical data (Nair et al., 2016; Kripa et al., 2018; Daniel and Thomas, 2022; Abdussamad et al., 2015; Henschke et al., 2018) and theoretical assumptions (Rohit et al., 2018; Annigeri, 1971). Details regarding data used for the estimation of parameters are discussed in Appendix A.3.

The data used for analysis included the annual total oil sardine catch (in tonnes), the total number of units of ring seine fishing gear operated during the year, the total number of days in the reference period during which fishing activity took place, and the monthly density of phytoplankton cells per litre. The fishing time was estimated by pooling the daily estimates from different sampling days in a month. All of the data used in this study was collected from secondary sources.

2.2 Procedure of Generalized Modeling

We will now discuss the procedure for formulating Generalized models. For this, the conceptual model was formalized into a generalized dynamical systems model, in which placeholder

functions represent the processes governing the dynamics of state variables (Lade et al., 2015). The relationship between each state variable and the different processes affecting them is represented through differential equations and algebraic relationships without specifying any functional form. Appendix A.5 presents an application of this methodology to an ecological model from the literature.

2.2.1 Identification of state variables

The selection of appropriate state variables is a key consideration in model development, with the recommendation being to choose variables that exhibit an appropriate time lag or function as a stock with a sufficient time span.

When it comes to interpretability, generalized modeling can benefit from the inclusion of additional state variables without significantly impacting tractability. Therefore, it is generally recommended to include candidate variables instead of omitting them (Massing and Gross, 2021). Although this may result in a large but sparse Jacobian matrix, they are often more desirable than small dense ones. This sparsity can simplify the analysis and interpretation of the system's dynamics, making it easier to identify important variables and understand their roles.

2.2.2 Generalized Model Equations

Let there be n state variables such that $X = \sum_{i=1}^{n} X_i e_i$ and m intermediate variables such that $Y = \sum_{i=1}^{m} Y_i e_i$. Here, e_i is the standard basis denoting the index of the state variable in state space.

The differential equations describing the generalized model can be written in the form

$$\dot{X}_i = \sum_j F_{ij}(X, Y) \; ; \qquad F : \mathbb{R}^{n+m} \to \mathbb{R}^n \, . \tag{2.1}$$

The model is also constrained by algebraic equations containing intermediate variables.

$$Y_i = \sum_j G_{ij}(X, Y) \; ; \qquad G : \mathbb{R}^{n+m} \to \mathbb{R}^m \, . \tag{2.2}$$

2.2.3 Normalization

For convenience, we normalize all the variables and functions describing different processes.

For a variable X_i, we define $x_i = \frac{X_i}{X_i^*}$, where X_i^* is value of variable at steady state. Similarly for a process $F(X)$, we define $f(x) = \frac{F(X)}{F^*}$ where $F^* = F(X^*)$.

This gives us normalized differential equations

$$\dot{x}_i = \sum_j \frac{f_{ij} F_{ij}^*}{X_i^*} \tag{2.3}$$

At steady state, $\dot{x}_i = 0$, $x^* = 1$ and all normalized processes run at rate 1. so, $\sum F_{ij}^* = 0$.

2.2.4 Jacobian matrix

Linearization is a technique that uses the Jacobian matrix to approximate the behaviour of a nonlinear system near an equilibrium point by a linear system. The Jacobian matrix of a dynamical system is a matrix of partial derivatives that describes the local behaviour of the system near an equilibrium point. The linear approximation of f around the equilibrium point is obtained by taking into account only the first-order terms in the Taylor expansion. The basic idea behind linearization is that for sufficiently small perturbations around an equilibrium point, a nonlinear system can be approximated by a linear system, which is much easier to analyze. This approximation is valid only for small perturbations around the equilibrium point, and for larger perturbations, the nonlinear behaviour of the system becomes important. Jacobian matrices provide us with formal means to study the stability of a system near a fixed point.

The Jacobian matrix of the differential equations is calculated symbolically and is written in terms of generalized parameters (α, β and elasticities). To redeem the calculation of generalized modeling outputs from the values of state variables at fixed points, we rescale each state variable to have a value of 1 at the steady state. This allows us to write each element in the Jacobian matrix as a sum of partial derivatives of each process corresponding to a state variable, which are then rewritten in terms of the elasticities of functions. By substitution, we can write the Jacobian matrix solely in terms of the generalized parameters

(α, β and elasticities). The jacobian matrix of the state equations is of the form

$$
\mathbf{J}_{i,j} =
\begin{bmatrix}
\frac{\partial \dot{x}_1}{\partial x_1} & \frac{\partial \dot{x}_1}{\partial x_2} & \cdots & \frac{\partial \dot{x}_1}{\partial x_n} \\
\frac{\partial \dot{x}_2}{\partial x_1} & \frac{\partial \dot{x}_2}{\partial x_2} & \cdots & \frac{\partial \dot{x}_2}{\partial x_n} \\
\vdots & \vdots & \vdots & \vdots \\
\frac{\partial \dot{x}_i}{\partial x_1} & \frac{\partial \dot{x}_i}{\partial x_2} & \cdots & \frac{\partial \dot{x}_i}{\partial x_n}
\end{bmatrix}
$$

Each row of the jacobian matrix corresponds to a state variable and can be written as

$$
J_i = \sum_{k=1}^{n} \frac{\partial \dot{x}_i}{\partial x_k} e_k = \sum_{k=1}^{n} \left(\sum_j \frac{F_{ij}^*}{X_i^*} \frac{\partial f_{ij}}{\partial x_k} e_k \right) \tag{2.4}
$$

Now, the terms in jacobian can be rewritten in terms of generalized parameters. The elasticity parameter (exponent parameter) is defined as, $\eta(A, B) = \frac{B}{A} \frac{\partial A}{\partial B} \big|_*$. They are the logarithmic derivatives of the original functions. Apart from being easy to interpret, elasticities provide a measure of nonlinearity that can be very robustly estimated using limited and noisy data. So row of jacobian matrix at steady state is,

$$
J_i = \sum_{k=1}^{n} \left(\sum_j \frac{F_{ij}^*}{X_i^*} \frac{f_{ij}^*}{x_k^*} \eta(f_{ij}, x_k) e_k \right) = \sum_{k=1}^{n} \left(\sum_j \frac{F_{ij}^*}{X_i^*} \eta(f_{ij}, x_k) e_k \right) \tag{2.5}
$$

Define alpha parameter (turnover parameter), $\alpha_i = \frac{C}{X_i}$, where C is some combination of different functions. Now J_i is,

$$
J_i = \sum_{k=1}^{n} \left(\sum_j \alpha_i \frac{F_{ij}^*}{C_i} \eta(f_{ij}, x_k) e_k \right) \tag{2.6}
$$

Finally, the beta parameter is introduced as the fraction of the positive(negative) influence of a function representing a process. $\beta(F_{ij}^+) = \frac{F_{ij}^{+*}}{\sum_{j+} F_{ij}^{+*}}$. Also, at steady state, $\sum F_{ij}^+ = \sum F_{ij}^-$. Hence,

$$
\begin{aligned}
J_i &= \sum_{k=1}^{n} \left(\sum_{\forall F_{ij}>0} \alpha_i \frac{\beta(F_{ij}^+) \sum_j F_{ij}^{+*}}{C_i} \eta(f_{ij}, x_k) e_k + \sum_{\forall F_{ij}<0} \alpha_i \frac{\beta(F_{ij}^-) \sum_j F_{ij}^{-*}}{C_i} \eta(f_{ij}, x_k) e_k \right) \\
&= \sum_{k=1}^{n} \left(\frac{\alpha_i}{\beta(C_i)} \sum_j \beta(F_{ij}) \eta(f_{ij}, x_k) e_k \right).
\end{aligned} \tag{2.7}
$$

Notably, we are not forced to make assumptions about aspects of the system about which we are typically uncertain, such as the precise form of the Lotka-Volterra Predator-Prey Model (Lotka, 1925). In contrast, many more plausible structural features can be represented.

2.2.5 Intermediate variables

In addition to state variables, other intermediate variables can also be identified to be included in the model. They can be helpful in constraining the generalized model and limiting the ranges of generalized parameters. We will outline a method for deriving the relationship between different parameters from the algebraic relationships between different variables, which can then be used to substitute variables in the Jacobian matrix. By doing so, we can eliminate redundancy in the matrix and simplify our analysis.

An intermediate variable can be expressed in terms of algebraic relationships between functions of all variables. Normalized equation of an intermediate variable, $y_i = \sum_j \frac{g_{ij}(y)G_{ij}^*}{Y_i^*}$ i-th row of derivative matrix of Y can be written as

$$\tilde{J}_i = \sum_{k=1}^{n} \frac{\partial y_i}{\partial x_k} e_k \tag{2.8}$$

Derivatives can be written as

$$\frac{\partial y_i}{\partial x_k} = \sum_j \frac{G_{ij}^*}{Y_i^*} \frac{\partial g_{ij}}{\partial x_k} \tag{2.9}$$

So,

$$\begin{aligned}
\tilde{J}_i &= \sum_{k=1}^{n} \left(\sum_j \frac{G_{ij}^*}{Y_i^*} \frac{\partial g_{ij}}{\partial x_k} \right) e_k = \sum_{k=1}^{n} \left(\sum_j \frac{G_{ij}^*}{Y_i^*} \frac{g_{ij}^*}{x_k^*} \eta(g_{ij}, x_k) \right) e_k \\
&= \sum_{k=1}^{n} \left(\sum_j \beta(G_{ij}) \eta(g_{ij}, x_k) \right) e_k = \sum_{k=1}^{n} \eta(y_i, x_k) e_k
\end{aligned} \tag{2.10}$$

2.3 Model Overview

We formulated an elaborate social-ecological model to examine the involvement of various processes and mechanisms that could have contributed towards the emergence of a regime shift in sardine fisheries in Kerala. We relied on literature available to us from the ICAR-Central Marine Fisheries Research Institute (CMFRI), Kochi and other fisheries journals.

A conceptual model was initially developed, which represents the interrelationships and feedback loops between different variables and factors that influence the behaviour of the fisheries system, and it was visualized in the form of a causal loop diagram (Figure 2.1). Further details regarding the construction of this diagram are available in Appendix A.1.
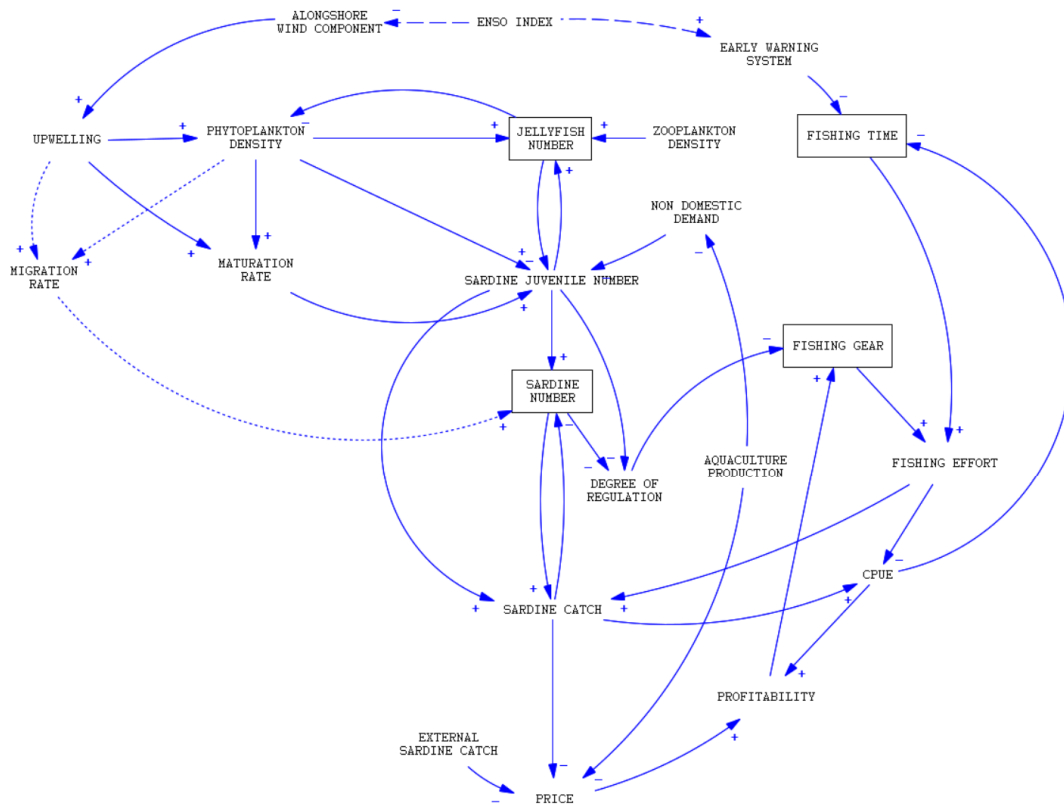

Figure 2.1: **Causal Loop Diagram.** Conceptual representation of the Indian Oil Sardine fisheries model. Here, dotted lines represent potential model experiments, and dashed lines represent ENSO teleconnections. Boxes indicate state variables of the system.

We incorporated three distinct subsystems in our model, each with a specific focus: the

ecological subsystem, which captures the biotic and abiotic components of the ecosystem; the fishing-related subsystem, which represents the behaviour and actions of fishers in the system; and the market economy-related subsystem, which accounts for the economic forces and market dynamics that influence the system.

2.4 Model Description of the IOS Fisheries System

The state variables involved in IOS fisheries model are *Sardine Number, Jellyfish Number, Fishing Gear* and *Fishing Time.* To capture the dynamic behaviour of the system, we developed a set of ordinary differential equations that describe how each variable changes as a function of its own state and the state of other variables in the model. Conventional models use precise and exact rules and equations to govern variables based on given initial conditions. However, we have not constrained the functions used in our ordinary differential equations, but we have assumed that the gains and losses between variables can be represented by mathematical functions. In some cases, it may not be directly informative to rely solely on the causal loop diagram to understand how variables change when processes depend on the variable itself. For example, in Equation (2.12), the variable jellyfish number may depend on itself through processes such as strobilation, senescence, and mortality.

We will now delve deeper into the model's components by discussing the ordinary differential equations used to capture the system's dynamic behaviour in Subsection 2.4.1. We will also explore the algebraic relationships between variables in Subsection 2.4.2, which govern the way variables interact with each other. In Subsection 2.4.3, we will analyze the stability of the system using the Jacobian matrix, and in Subsection 2.4.4, we will discuss the use of generalized parameters to simulate different scenarios. By examining each of these components in detail, we can gain a comprehensive understanding of the IOS fisheries model.

2.4.1 Differential equations of the State Variables

In the Generalized modeling framework, we do not restrict the processes in the model to specific functional forms, and thus we cannot meaningfully compute the steady states of the model. However, under assumptions that the state variables change due to various gain and

loss functions, we can write the ordinary differential equations (ODEs) of the system. In this section, we will describe each equation governing the dynamics of the fisheries system.

Sardine Number   Oil sardine grows rapidly, matures early, and a few continue to survive beyond 18 months (Longhurst and Wooster, 1990). The increase in the sardine population number is represented by the sardine recruitment function and migration process function. Here, by convention, we consider the (inward) migration function to be positive based on a schematic map portraying the distribution and migration pattern of Indian Oil Sardine, which can be found in the CMFRI Newsletter (CMFRI, 2007). The decrease in the sardine population number is represented by the sardine mortality and the sardine catch.

$$
\begin{aligned}
\frac{d}{dt}(SardineNumber) = &\ SardineReruitmentIntoAdult(SardineJuvenileNumber) - SardineCatch \\
&- SardineMortalityNumber(SardineNumber) + MigrationNumber(MigrationRate)
\end{aligned}
$$

$$(2.11)$$

Jellyfish Number   Jellyfish play a critical role in the functioning of marine ecosystems by supporting various processes and trophic interactions. These macro-plankters primarily prey on zooplankton and fish larvae and are known to affect fish recruitment (Lynam et al., 2005). Jellyfish blooms were seen in the inshore surface and column waters of the primary sardine fishing area from 5 to 30 m depth zone in June 2013 and August to September 2014 (Kripa et al., 2018). Jellyfish undergo a complex life cycle that involves an alternation of generations between a sexual medusa stage and an asexual polyp stage. Polyps can undergo strobilation, where they divide into stacked disks that develop into juvenile medusae. Adult medusae eventually undergo senescence. We used a pre-existing Scyphozoan jellyfish model (Henschke et al., 2018) to incorporate medusa dynamics and strobilation.

$$
\begin{aligned}
\frac{d}{dt}(JellyfishNumber) = &\ JellyFishMedusaStrobilation(JellyFishNumber) \\
&+ JellyFishGrowth(PhytoPlanktonDensity, ZooPlanktonDensity, SardineJuvenileNumber) \\
&- JellyFishSenescence(JellyFishNumber) - JellyFishPredationMortality(JellyFishNumber)
\end{aligned}
$$

Fishing Gear   Modernisation of fisheries in Kerala has increased fishing effort and catch since areas beyond conventional fishing grounds were also explored. We modeled two major types of gears (Inboard ring seine and Outboard ring seine), which together account for 90% of the oil sardine catch (Abdussamad et al., 2015), separately, due to the difference in their efficiencies. Heterogeneities in the fishing gear beyond the distinction between OBRS and IBRS were not modeled. We also accounted for the potential loss of fishing gear due to abandonment, market exit, or discarding, which may result in a decrease in the overall fishing gear size. We kept the proportional gear exit same for all years (i.e., linear gear exit *w.r.t* total annual fishing gear size)

$$
\frac{d}{dt}(FishingGear) = FishingGearOBRS(Profitability) + \ FishingGearIBRS(Profitability) \\
- \ GearExit(FishingGear, DegreeOfRegulation)
$$

(2.13)

Fishing Time   We modeled fishers as satisficers (Simon, 1955) who engage in income- or yield-targeting, whereby fishers adjust their fishing time according to Catch per unit effort on a particular timescale instead of trying to maximize intertemporal profits (Nguyen and Leung, 2013). Extreme weather events have led to challenges like loss in fishing time and false alarms affecting fisher livelihood (Martin et al., 2022). Hence, we considered the loss in fishing days in the model.

$$
\frac{d}{dt}(FishingTime) = \ FishingTime - FishingCompensatedTime(CPUE) \\
- LossInFishingTime(EarlyWarningSignals)
$$

(2.14)

2.4.2 Algebraic relationships of Intermediate Variables

Ecosystem Dynamics   Oil sardines are primarily planktivores (i.e., they feed on plankton). Important ecological variables such as phytoplankton density and Jellyfish (predator) number were included to capture prey-predator dynamics affecting the sardine population. The juvenile sardine fish population was modeled separately since they are directly linked to the regulation of fishing due to excessive capture of the spawning stock. Upwelling is a driver that influences the maturation and migration of sardines (Kripa et al., 2018) and is believed to play a vital role in the variability of the sardine stock. Upwelling is known to significantly impact phytoplankton density by bringing nutrient-rich water to the surface, thereby increasing the availability of essential nutrients for phytoplankton growth. The alongshore wind component plays a crucial role in driving upwelling by pushing surface waters away from the shore and allowing nutrient-rich, cooler water to rise to the surface. The intensity and direction of the alongshore wind component can influence the strength of upwelling (Muni Krishna, 2008). ENSO (El Niño-Southern Oscillation) also impacts upwelling (Kripa et al., 2018) by altering the wind patterns in the equatorial Pacific. However, it was not considered in the model equations since it is merely a teleconnection (Achuthavarier et al., 2012) and not a causal link. Since variables represent

$$
\begin{aligned}
MigrationRate &= Migration(Upwelling, PhytoPlanktonDensity) \\
MaturationRate &= SardineMaturation(Upwelling, PhytoPlanktonDensity) \\
SardineJuvenileNumber &= SardineJuvenileGrowth(MaturationRate, PhytoplanktonDensity) \\
&\quad - JuvenileCatchRate(NonDomesticDemand) \\
&\quad - JuvenileMortality(JellyFishNumber) \\
PhytoPlanktonDensity &= PhytoPlanktonGrowth(Upwelling) \\
&\quad - PhytoPlanktonConsumptionJellyfish(JellyFishNumber)
\end{aligned}
$$

Social Dynamics   We modeled sardine adult catch and juvenile catch separately to study the impact of juvenile fishing on the system. Fishing effort is directly proportional to fishing gear and fishing time. CPUE, which represents the amount of sardine catch per unit of fishing effort, is also directly proportional to the fishing effort. The elasticities for the links associated with these intermediate variables will be 1.

$$
\begin{aligned}
SardineCatch \quad &= SardineAdultCatch(SardineNumber, FishingEffort) \\
&+ SardineJuvenileCatch(SardineJuvenileNumber, FishingEffort) \\
FishingEffort \quad &= FishingEffortOBRS(FishingGearOBRS, FishingTime) \\
&+ FishingEffortIBRS(FishingGearIBRS, FishingTme) \\
CPUE \quad &= CPUE(SardineCatch, FishingEffort)
\end{aligned}
$$

Market Economics and Regulations   Fishing behaviour is directly linked to market
dynamics (price, profitability) through feedback loops. We modeled market price of sardine
fish as a function of local sardine catch and total substitutable commodity (external sardine
catch and aquaculture production). We did not consider other commonly available fish as
substitutable. Consumer preference plays an important role in stability and management of
multispecies fisheries (Quaas and Requate, 2013). Juvenile fishing, which was more prevalent
during the early 2010s, increased in response to non-domestic demand (Shyam et al., 2015)
from fishmeal and bait industries (Mohamed et al., 2014). We considered this in our model
by modeling juvenile fish population separately.

$$
\begin{aligned}
Price \quad &= Price(SardineCatch, ExternalSardine, AquacultureProduction) \\
Profitability \quad &= MarginalReturn(CPUE, Price) \\
DegreeOfRegulation \quad &= DegreeOfRegulation(SardineNumber, SardineJuvenileNumber) \\
NonDomesticDemand \quad &= NonDomesticDemand(AquacultureProduction)
\end{aligned}
$$

Note that the variables in question are constrained to be greater than or equal to zero (i.e.,
$X_1, X_2, ..., X_n, Y_1, Y_2, ..., Y_m \geq 0$), as they correspond to the measurement of non-negative
real quantities.

2.4.3   Symbolic representation of the jacobian matrix

In the case of Indian Oil Sardine (IOS) fisheries, we assume the existence of a fixed point
by looking at a short time period of the IOS stock, thus considering local stability. We
may neglect the impact of slow variables on the value of the fixed point. This assumption
allows us to use the Jacobian matrix to analyze the stability of the system around this fixed
point. Specifically, we have used Equation (2.7) to derive the symbolic representation of the
Jacobian matrix, which provides insights into the system's behaviour near the fixed point.
The 4x4 Jacobian matrix displays the first-order partial derivatives of a vector function with

respect to the variables Sardine Number, Jellyfish Number, Fishing Gear, and Fishing Time as the columns of the matrix, with each row specifying the corresponding variable. The variable order in the matrix is significant, as changing it would result in a different Jacobian matrix.

The jacobian matrix for our model can be written as

$\alpha_{SN} \cdot ((1 - \beta_{MN}) \cdot \eta[SRIA, SN] - \beta_{SC} \cdot \eta[SC, SN] - (1 - \beta_{SC}) \cdot \eta[SMN, SN])/\beta_{SMN}$	$\alpha_{SN} \cdot ((1 - \beta_{MN}) \cdot \eta[SRIA, JFN] + \beta_{MN} \cdot \eta[MN, JFN] - \beta_{SC} \cdot \eta[SC, JFN] - (1 - \beta_{SC}) \cdot \eta[SMN, JFN])/\beta_{SMN}$	$\alpha_{SN} \cdot (\beta_{SC} \cdot \eta[SC, FG])/\beta_{SMN}$	$\alpha_{SN} \cdot (\beta_{SC} \cdot \eta[SC, FT])/\beta_{SMN}$
$\alpha_{JFN} \cdot (\beta JFG \cdot \eta[JFG, SN])/\beta_{JFS}$	$\alpha_{JFN} \cdot (\beta_{JFMS} \cdot \eta[JFMS, JFN] - \beta_{JFPM} \cdot \eta[JFPM, JFN] - \beta_{JFS} \cdot \eta[JFS, JFN])/\beta_{JFS}$	0	0
$\alpha_{FG} \cdot (\beta_{FGOBRS} \cdot \eta[FGOBRS, SN] + \beta_{FGIBRS} \cdot \eta[FGIBRS, SN] - \beta_{GE} \cdot \eta[GE, SN])/\beta[GE]$	0	$\alpha_{FG} \cdot (\beta_{FGOBRS} \cdot \eta[FGOBRS, FG] + \beta_{FGIBRS} \cdot \eta[FGIBRS, FG] - \beta_{GE} \cdot \eta[GE, FG])/\beta_{GE}$	$\alpha_{FG} \cdot (\beta_{FGOBRS} \cdot \eta[FGOBRS, FT] + \beta_{FGIBRS} \cdot \eta[FGIBRS, FT] - \beta_{GE} \cdot \eta[GE, FT])/\beta_{GE}$
$\alpha_{FT} \cdot (\eta[FT, SN] - \beta_{FCT} \cdot \eta[FCT, SN])$	0	$\alpha_{FT} \cdot (\eta[FT, FG] - \beta_{FCT} \cdot \eta[FCT, FG])$	$\alpha_{FT} \cdot (1 - \beta_{FCT} \cdot \eta[FCT, FT] - \beta_{LFT} \cdot \eta[LFT, FT])$

2.4.4 Generalized parameters

The generalized parameters are capable of representing a class of models rather than a specific one and can be easily interpreted based on domain knowledge. The α parameters determine the time scale of different state variables, which is defined by choosing a process or combination of processes and expressing it in proportion to the state variable. The β parameters indicate the relative influence of two processes on a state variable, which is defined as the ratio of the positive (negative) influence of a process with respect to all corresponding positive (negative) processes. It is noteworthy to observe that beta parameters appear in complementary pairs, as presented in Table 2.1. The presence of this inherent symmetry in the system enables easier calculation of relevant information, such as the Jacobian matrix, by reducing computational complexity. Additional information regarding the method by which this reduction is achieved can be found in section 2.2. Elasticities represent non-linearities of links, with a value of 1 corresponding to a linear relationship.

Based on data available to us and qualitative knowledge from literature, we assign values and ranges to these parameters for the time period from boom to the beginning of collapse (2010-2013). In instances where data for certain parameters during the boom period were not available, we opted to assign a uniform distribution ranging from 0 to 1.

Beta Parameter	Complementary Parameter	Contribution type
b_SRIA	b_MN	positive
b_SC	b_SMN	negative
b_JFG	b_JFMS	positive
b_JFPM	b_JFS	negative
b_FGOBRS	b_FGIBRS	positive
b_FCT	b_LFT	negative

Table 2.1: **Complementary beta parameters.** The existence of complementary parameters in our study is attributed to the equilibrium condition where the summation of all positive (negative) beta parameters corresponding to a state variable is equal to one.

2.5 Feedback loops

In dynamical systems, feedback loops refer to the circular causal relationships between the different components of the system (Sterman, 2010). There are two types of feedback loops: reinforcing and balancing. Reinforcing loops lead to exponential growth or decay in the system while balancing loops stabilize the system by counteracting changes. The sign of a feedback loop* can be mathematically defined using the product of the partial derivatives of the variables involved in the loop. A positive feedback loop reinforces the change in the variables, while a negative feedback loop balances the change and stabilizes the system. For an arbitrary feedback loop consisting of n variables, the polarity of loop $= \mathrm{SGN}\left(\dfrac{\partial x_1^O}{\partial x_1^I}\right) =$ $\mathrm{SGN}\left[\left(\dfrac{\partial x_1^O}{\partial x_n}\right)\left(\dfrac{\partial x_n}{\partial x_{n-1}}\right)\left(\dfrac{\partial x_{n-1}}{\partial x_{n-2}}\right)\cdots\left(\dfrac{\partial x_2}{\partial x_1^I}\right)\right]$, where x_1 splits into input x_1^I and output x_1^O. The feedback loops present in the model can be located in Appendix A.3 for reference.

2.6 Stability

The "instability" of the system is defined as the real part of the dominant eigenvalue of the Jacobian matrix. After assigning ranges to parameters, we sampled the parameter space using Latin hypercube sampling (LHS) (Jin et al., 2003), and the dominant eigenvalue of the jacobian matrix was computed for the entire class of models. Latin hypercube sampling is a statistical method for generating a quasi-random sampling distribution by dividing each variable's dimension space into n sections and placing only one point in each section. It is possible that the sampling might lead to positive eigenvalues even if the system has a stable state with a negative dominant eigenvalue. This is reasonable because the generalised model sometimes becomes unstable due to regime shifts. This can also happen due to statistical fluctuations in the sampled data or if the parameter space is highly nonlinear. Note that uncertainty ranges of unknown parameters were conservatively estimated (i.e., ranges of possible values for the parameters were chosen in a way that is deliberately wider or more inclusive in order to account for any potential errors or variations in the underlying data or assumptions). In any case, it is still valid to use the dominant eigenvalue as a measure of (in)stability. The dominant eigenvalue is just one measure of the system (in)stability.

---

*The sign of a feedback loop can be determined by counting the number of negative links; if the count is even, the loop is positive, and if it is odd, the loop is negative.

2.7 Model Validation

Sensitivity analysis tests were performed to determine the robustness and reliability of the model under different scenarios and identify any weaknesses or uncertainties in the model that need to be addressed. Sensitivity analysis is performed on dynamical system models to investigate how changes in the values of input parameters or initial conditions affect the behaviour of the system over time. By exploring the effects of parameter variations on the model output, sensitivity analysis can help to identify the most influential parameters and provide insights into how to improve the model. We performed One-At-a-Time (OAT) sensitivity analysis and Morris sensitivity analysis (Morris, 1991). In OAT method, a single parameter is varied while all other parameters are held constant, and the resulting changes in the output of the system are observed. Here, the output is the dominant eigenvalue of the jacobian matrix of the system. While OAT sensitivity analysis is a straightforward and commonly used method for identifying influential model inputs, it may fail to capture the complex and nonlinear relationships between parameters. In contrast, Morris sensitivity analysis evaluates the impact of multiple parameters by generating many random trajectories, each of which perturbs multiple parameters simultaneously. While only one parameter is varied along each trajectory, the method systematically explores the parameter space through a large number of trajectories, providing a more comprehensive understanding of parameter interactions and dependencies compared to OAT sensitivity analysis. A detailed description of the methodology for conducting Morris sensitivity analysis is presented in Appendix A.4.

2.8 System Details

The causal loop diagrams were made on Vensim PLE Version 9.3.2x64(x64). All numerical simulations were run on Ipython 8.2.0. The sampling of the dominant eigenvalues was done using `lhs` module of the `pyDOE` package v0.3.8 (Baudin et al., 2013) and `scipy` package v1.7.3 (Virtanen et al., 2020). The Morris sensitivity analysis was done using `SALib` package v1.4.5 (Iwanaga et al., 2022; Herman and Usher, 2017).

Chapter 3

Results and Discussion

This chapter presents the results and analysis of the IOS fisheries model. We will address key questions that were explored in this study, including the stability of the system, sensitivity analysis of generalized parameters of the system and scenario analysis. By examining these questions, we aim to provide a comprehensive understanding of the different components of the system and their impact on the qualitative state of the system in the context of fisheries regime change.

3.1 Is the generalized model stable at baseline?

The primary objective of the generalized modeling procedure is to evaluate (in)stability of the system near the equilibrium point. It cannot generate time series output and thus cannot be used for future prediction like a simulation model. Here, the "instability" of the system refers to the real part of the dominant eigenvalue of the Jacobian matrix. Figure 3.1 shows the distribution of the real part of dominant eigenvalues of the baseline class of systems, which includes both stable and unstable cases. This distribution represents different combinations of parameters belonging to various parameter ranges in the model class. The likelihood of parameter combinations is not explicitly known from the distribution, and it is not safe to assume that all parameter combinations are equally likely. However, a significant proportion of the parameter combinations in the model class result in a stable system with a negative real part of the dominant eigenvalue.
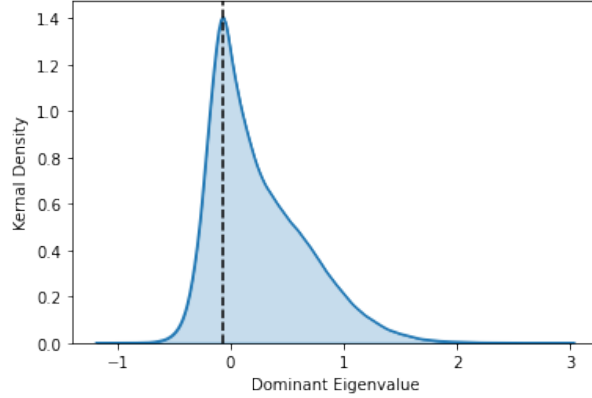
Figure 3.1: **Distribution of instability.** Kernal density of distribution of dominant eigen-values for the baseline class of models estimated from a Latin hypercube sampling simulation with $n = 6 \times 10^6$ samples (positive/negative numbers indicate an unstable/stable system). The maximum distribution density is at eigenvalue = -0.061.

3.2 Which generalized parameters are sensitive to perturbations?

Observation 1. Among the beta parameters, the one associated with sardine recruitment and migration has the most significant impact on system stability.

This parameter is particularly important given the spatial distribution of Indian Oil Sardine migration, which ranges from the Gulf of Oman to the Malabar coast, with different coastal niches playing a crucial role in stock abundance. Previous research has emphasized the need for a better understanding of stock migration to manage the stock effectively (Kripa et al., 2018). The sensitivity of β_{SRIA} at baseline is $\mu^* = 0.2909$ with 95% confidence interval $= 0.003338$ and $\sigma = 3.312e - 01$.

Observation 2. The beta parameter related to fishing gear type β_{FGOBRS} has a negligible effect on the stability.

During the fisheries boom, the contribution of outboard ring seine (OBRS) fishing gear declined from 73% in 2007 to 33% in 2012, just before the collapse of fisheries. However, in the aftermath of the fishery collapse, the aforementioned contribution quickly surged to 63% in 2014. We decided to test the effect of fishing gear heterogeneity on the stability of the

28

system and found that at baseline, β_{FGOBRS} has the least sensitivity among beta parameters ($\mu^* = 0.01046$ with 95% confidence interval $= 0.0001495$ and $\sigma = 1.824e - 02$).

Observation 3. The elasticity (degree of nonlinearity) of fishing time with respect to sardine number and elasticity of fishing compensated time with respect to sardine number are the most sensitive parameters.

A key assumption about fishing behaviour was that fishers are satisficers and therefore were likely to increase(decrease) time spent fishing with decreasing(increasing) $CPUE$ (Simon, 1955). The assumption suggests that there will be negative feedback from $CPUE$ to $fishing\ time$. The sensitivity values also have high uncertainty ($\eta[FCT, SN] : \mu^* = 0.8273$ with 95% confidence interval $= 0.005641$ and $\sigma = 5.239e - 01$; $\eta[FT, SN] : \mu^* = 0.8915$ with 95% confidence interval $= 0.006095$ and $\sigma = 5.494e - 01$).
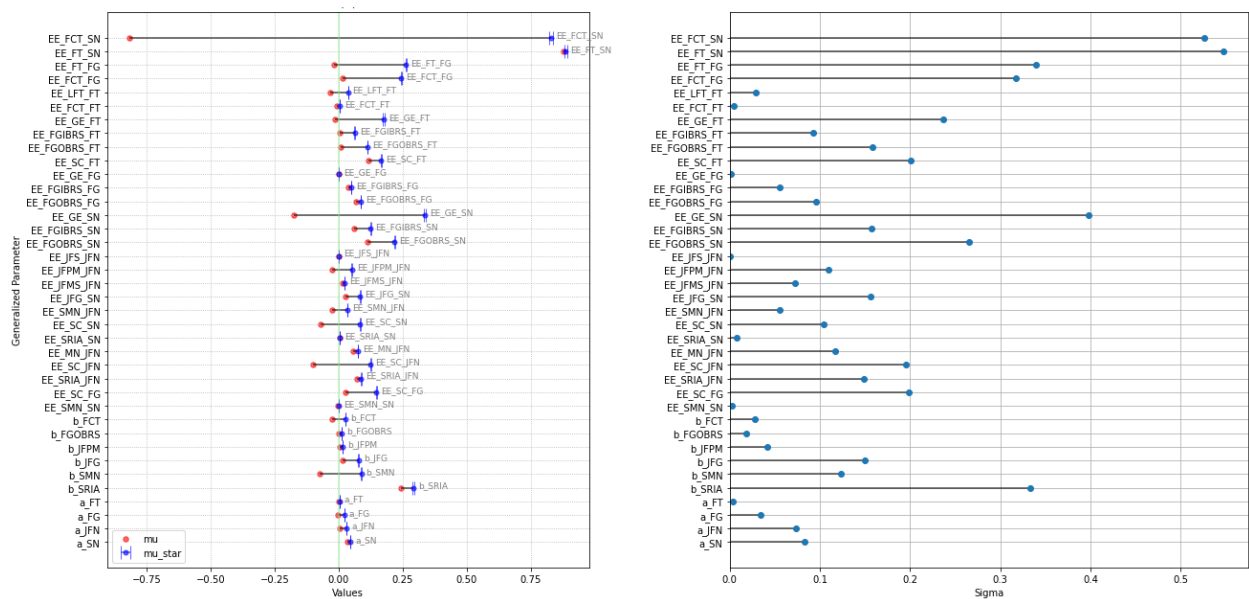
(a) Sensitivity values of parameters at baseline

(b) Variance of Sensitivity values of parameters at baseline

Figure 3.2: **Morris SA test at baseline** (a) The red dot denotes the net direction of sensitivity (μ) and the navy blue dot denotes the average value of absolute sensitivity (μ^*). (b) The σ values tell us about the variance or how the sensitivity value of a parameter depends on choice of other parameters.

3.3 The effect of sardine migration

We explored how the sensitivity of different parameters changed under different migration scenarios. The migration we considered is inward migration during peak recruitment season. Sardine migration and recruitment were assumed to be positive processes that contribute to an increase in the sardine population. We adjusted the range of the beta parameter β_{SRIA} (which is complementary to the migration beta parameter β_{MN}) to (0,0.33] for high migration and [0.67,1) for low migration. Sensitivity analysis was performed under both scenarios.

Observation 4. β_{SRIA} is the most sensitive parameter under the high recruitment(low migration) scenario ($\mu = 1.8986, \mu^* = 1.8988$).

Figure 3.3a and Figure 3.4a demonstrate how the tradeoff between sardine population increase resulting from migration and recruitment impacts stability under perturbations under both scenarios. Note that $\beta_{SRIA} = 1 - \beta_{MN}$. Reduced fish migration may be attributed to variability in SST and upwelling conditions (Muni Krishna, 2008).

Observation 5. The overall uncertainty in the model increases under the high recruitment(low migration) scenario.

The variance associated with the sensitivity of β_{SRIA} changes from $\sigma(\beta_{SRIA} \mid 0 < \beta_{SRIA} < 0.33) = 1.1062e{-}01$ to $\sigma(\beta_{SRIA} \mid 0.67 < \beta_{SRIA} < 1) = 8.74741e{-}01$. The variance associated with sensitivity of fishing time-related elasticity parameters $\sigma(\eta[FT, SN] \mid 0 < \eta[FT, SN] < 0.33) = 2.7245e - 01$ increases to $\sigma(\eta[FT, SN] \mid 0.67 < \eta[FT, SN] < 1) = 8.7627e - 01$ and $\sigma(\eta[FCT, SN] \mid 0 < \eta[FCT, SN] < 0.33) = 2.6044e{-}01$ increases to $\sigma(\eta[FCT, SN] \mid 0.67 < \eta[FCT, SN] < 1) = 8.5053e{-}01$.It is noteworthy that comparable increments are noticeable across various parameters. Figure 3.3b and Figure 3.4b shows uncertainty associated with different parameters under both scenarios.
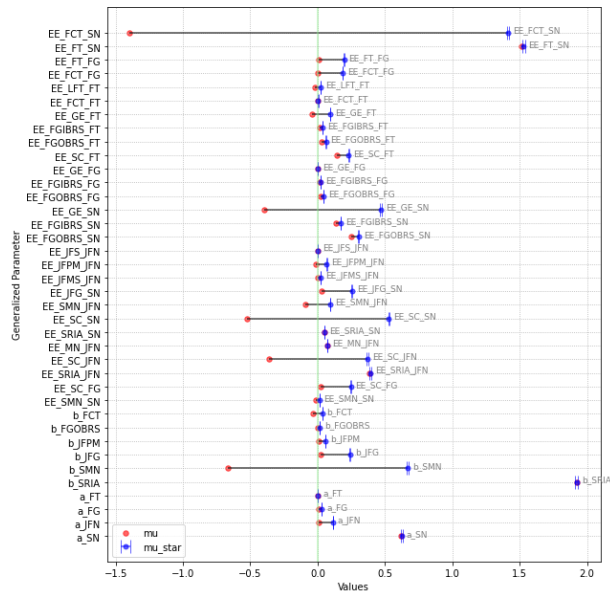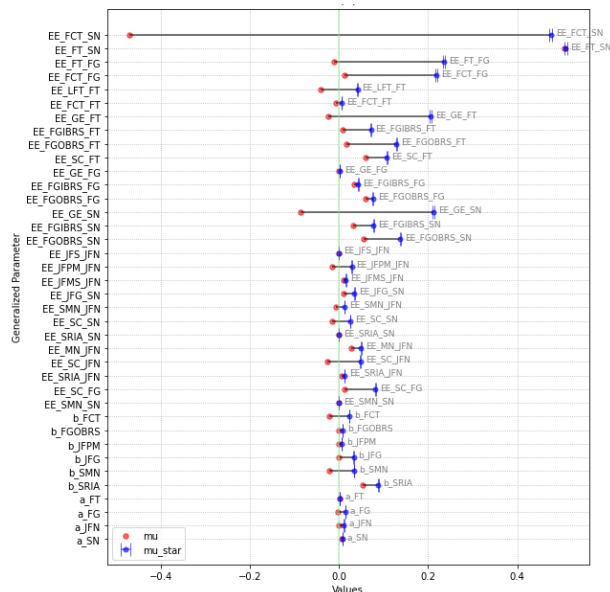
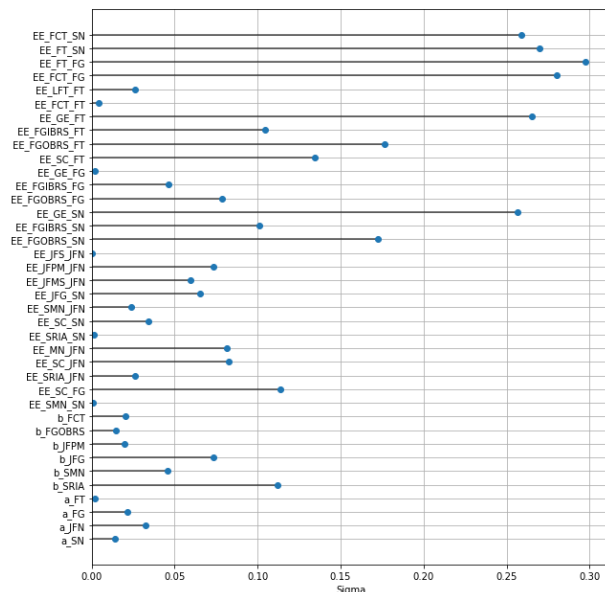(a) Sensitivity values of parameters at high b_SRIA scenario
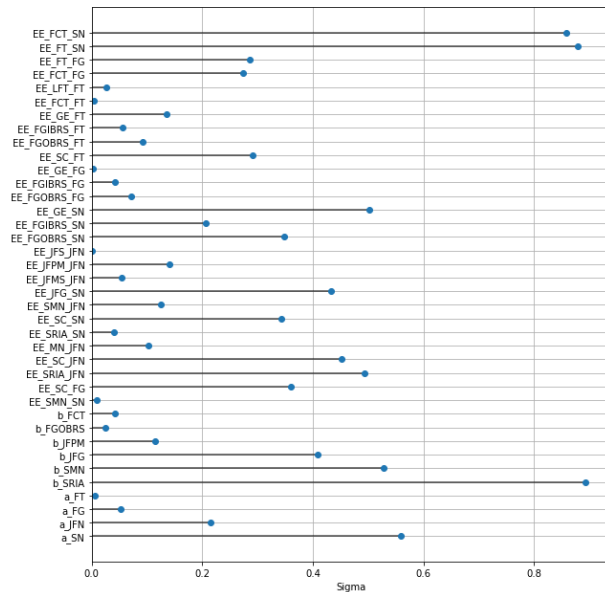
(b) Variance of Sensitivity values of parameters at high b_SRIA scenario

Figure 3.3: **Morris SA test at at high b_SRIA scenario**

(a) Sensitivity values of parameters at low b_SRIA scenario

(b) Variance of Sensitivity values of parameters at low b_SRIA scenario

Figure 3.4: **Morris SA test at at low b_SRIA scenario**

3.4 What are the tipping points of the system?

Bifurcation-induced tipping, also known as B-tipping, occurs when a parameter shift, such as a change in environmental conditions, reduces the basin of attraction of the original stable state to zero (Ashwin et al., 2012). Figure 3.5a and Figure 3.5b in the context shows fold bifurcation points for the alpha parameters and beta parameters resulting from a One-At-a-Time analysis respectively. However, given that other factors are always at play (*ceteris is never paribus*), the observed fold bifurcation points might be influenced by external variables or unknown factors, leading to a deviation from the actual tipping points of the system.

Observation 6. An interesting observation for the specific case we examined is that the complementary beta parameters associated with recruitment and migration (β_{SRIA} & β_{MN}) have two bifurcation points at $\beta_{SRIA} = 0.29$, $\beta_{SRIA} = 0.56$. The system remains stable solely within this range. Appendix A.3 lists the parameters used for this case.

3.5 How do changes in the elasticities between intermediate variables impact the stability of the system?

The relationship between elasticity parameters of different state and intermediate variables is expressed in Equation (2.10). This relationship can help us understand how the magnitude of sensitivity of the intermediate variable elasticity is constrained by the sensitivity values of state variables. Specifically, if η represents elasticity and f is a function that takes either an intermediate y or state variable x, then the elasticity of f with respect to an intermediate variable x can be expressed as $\eta(f(x), x) = \eta(f(y), y) \cdot \eta(y(x), x)$. However, this relationship does not offer a straightforward indication of the direction of the change.

When $0 < \eta < 1$, the sensitivity of the elasticity of an intermediate variable is bounded by the sensitivity of the corresponding elasticity of a state variable. Table 3.1 provides specific information on the elasticities related to select intermediate variables of interest.

Observation 7. By definition, $\eta[CPUE, FG] = 1$ in Table 3.1. Therefore, $\eta[FCT, FG] = \eta[FCT, CPUE]$ ($\mu(\eta[FCT, FG]) = 4.1565e-03$; $\mu^*(\eta[FCT, FG]) = 0.2029$; $\sigma(\eta[FCT, FG]) =$

$2.8862e - 01$).

The elasticities have equal magnitudes, resulting in an equivalent absolute sensitivity μ^*. However, increasing the fishing gear will cause a linear increase in fishing effort and a subsequent linear decrease in CPUE, resulting in an opposite direction of sensitivity. This means that an increase in $\eta[FCT, CPUE]$ will have a stabilizing effect on the system. If fishers sufficiently adjust their fishing time in response to an increase in CPUE, the system may strengthen stability.

Intermediate variable	Comments	Elasticity Parameter (η)
Phytoplankton(PHY)	Onset of collapse PHY density increased	$\eta[SRIA, JFN] = \eta[SRIA, SJN] \cdot \beta_{SJG} \cdot \eta[SJN, PHY] \cdot \beta_{PPCJ} \cdot \eta[PHY, JFN]$
Degree of Regulation(DOR)	How strict and enforced is regulation	$\eta[FGOBRS, SN] = \eta[FGOBRS, DOR] \cdot \eta[DOR, SN]$
		$\eta[FGIBRS, SN] = \eta[FGIBRS, DOR] \cdot \eta[DOR, SN]$
Catch Per Unit Effort(CPUE)	Increased for both OBRS and IBRS gears till 2011 and 2012 respectively and then decreased	$\eta[FCT, SN] = \eta[FCT, CPUE] \cdot \eta[CPUE, SN]$
		$\eta[FCT, FG] = \eta[FCT, CPUE] \cdot \eta[CPUE, FG]$

Table 3.1: **Summary of Intermediate variables.** Elasticities between different variables are determined by the chain rule, which does not capture the direction of change as elasticity is always positive by convention. However, elasticities can provide valuable information about the sensitivity of a system to changes in its variables. This sensitivity can be quantified by taking the partial derivative of the system output, such as instability, with respect to the elasticity parameter. By doing so, we can gain insight into how changes in one parameter may affect the overall system and its stability.
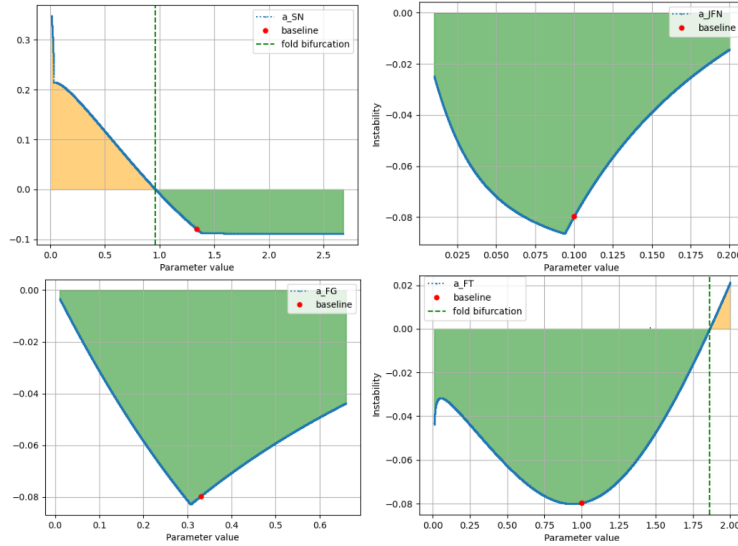
(a) Response of alpha (α) parameters to perturbation from baseline. Green(orange) shade indicate stable(unstable) region.
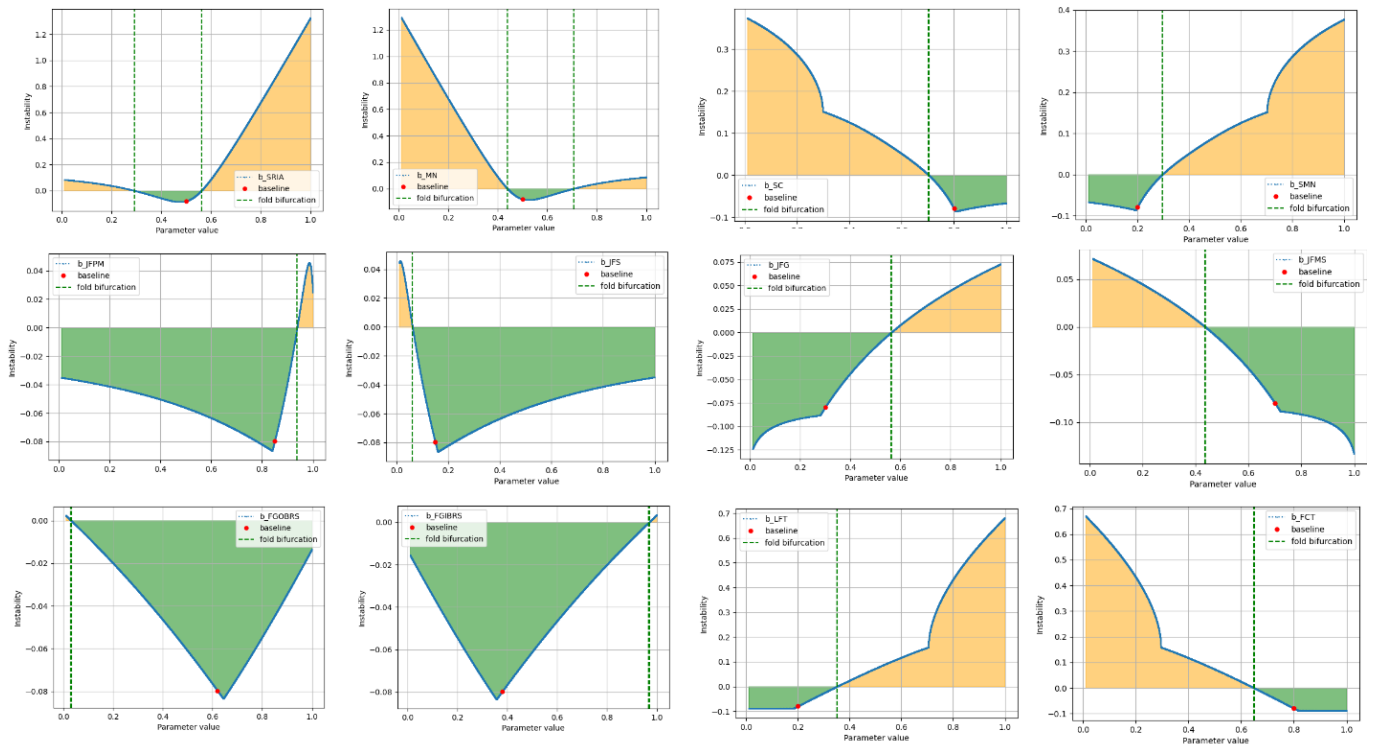
(b) Response of beta (β) parameters to perturbation from baseline. Green(orange) shade indicate stable(unstable) region.

Figure 3.5: **Response curves of parameters.** The parameter values used for this analysis are given in Table A.1. A number of parameters exhibit fold bifurcation points, denoted by a vertical dashed line.

34
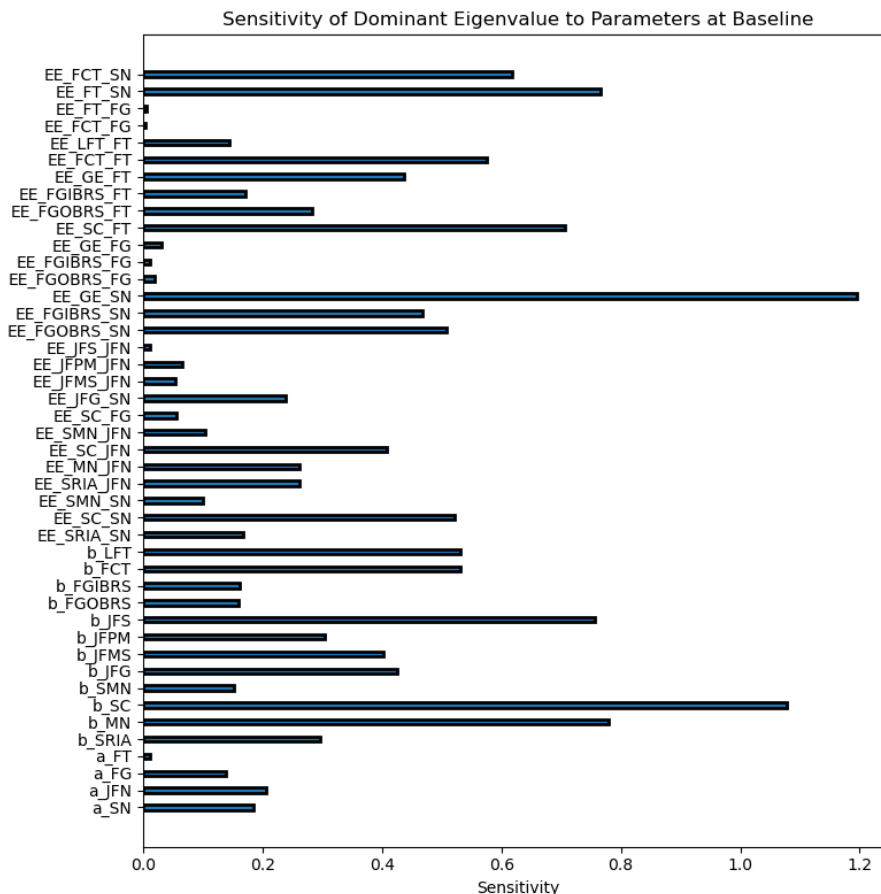
Figure 3.6: **One-At-a-Time Sensitivity Analysis.** Sensitivity values of parameters at baseline stability, obtained by calculating the local derivative within an $\epsilon = 0.01$ neighbourhood around the baseline values while keeping the index number consistent for both the numerator(output) and denominator(input). Here, the output is the dominant eigenvalue of the jacobian, and the input is the parameter value.

3.6 Is the generalized model a valid representation of the system?

Unfortunately, it is impossible to define a prediction loss function to validate our model. However, we can use our knowledge of the Indian Oil Sardine fishery's known features to assess the validity of our model by examining how various parameters change from the period of relative abundance preceding the collapse to the onset of the collapse. As previously

explained, the onset of a collapse is marked by a decline in the stability of the system's previous qualitative state (or an increase in the dominant eigenvalue of the jacobian associated with that state). This implies that parameters with positive(negative) μ values should increase(decrease) in value.

Based on data available from CMFRI- NMFDC database, the total catch of sardine fish in Kerala increased from 259342 tonnes in 2010 to 399786 tonnes in 2012. The beta parameter associated with sardine catch and sardine natural mortality tradeoff, β_{SMN} decreased as a result. Figure 3.2 depicts the direction of μ associated with this parameter. Similar validation can be done for all parameters provided data is available to us to verify the direction of change. The present study faced significant limitations due to the insufficient frequency of temporal data.

Chapter 4

Conclusion and Outlook

In this work, we found that fish migration can have a major influence on the socio-ecological dynamics of the Indian Oil Sardine fisheries. In particular, we investigated how the influence of various parameters on stability changes under different scenarios of fish migration. Our findings indicate that low fish migration intensifies uncertainty in the fisheries system and makes it more vulnerable to changes in other parameters. Investigating the interplay between the effect of inward fish migration and fishing behaviour revealed an important trade-off parameter.

When the degree of nonlinearity(elasticity) associated with fishing time and fishing compensated time $w.r.t$ sardine number changes, it significantly affects the stability of the system. However, the uncertainty associated with the sensitivity of these parameters is also high. This could be due to uncertainty in the way fishing time is modeled (structural uncertainty), which is reflected in the variance (σ) of sensitivity values of these parameters. A comprehensive understanding of the role of fisher behaviour in stabilizing fisheries systems requires a nuanced approach that incorporates the complexities of fisher behaviour. Therefore, further research is needed to elucidate the various behavioural aspects and their effects on the functioning of fisheries systems. Such insights can inform the development of effective policies aimed at promoting sustainable fisheries management.

In this work, we assumed that variations in the elasticity values of fishing gear would result in differing effects on system stability. To model this heterogeneity, we incorporated these differences into our model. However, we found that changes in gear type did not

significantly affect the model at baseline calibration.

Although quantitative data is not always necessary to construct a dynamical systems model, conceptual models often rely on extensive literature review and expert input. While system behaviour can be explored through different analyses, the limitations of conceptual models must be acknowledged. Therefore, we recognize the uncertainty associated with the model structure. We must be cautious while using mathematical models for prediction, control and optimization in the paradigm of evidence based policy. Sensitivity auditing (Saltelli et al., 2013) applies sensitivity analysis as it is used in mathematical modeling to settings where the models are used to generate policy inference.

Generalized modeling can integrate knowledge from different domains and is well suited in a collaborative setting. However, choosing the right model requires careful consideration of the trade-offs between complexity, tractability, reproducibility and generalizability (Biggs et al., 2021) . It is important to assess the suitability of different models for the task at hand and to be transparent about the assumptions and limitations of the chosen model.

In conclusion, dynamical systems modeling is a powerful approach for studying complex systems, but it is important to combine it with other approaches or perspectives to gain a more comprehensive understanding of the system under investigation. By doing so, researchers can develop more effective and robust models, identify key drivers of change within the system, and gain a better understanding of the underlying social, ecological, and cultural factors that influence the system.

Appendix A

Appendix

A.1 Construction of the causal loop diagram(CLD)

Let f be a function that represents a causal link between two variables in a CLD. All the functions are defined such that $\frac{\partial |f|}{\partial x_k} > 0$. The polarity of the link can be determined by the sign of the function, denoted as $sgn(f)$. Specifically, if $sgn(f) > 0$, the link has a positive polarity, indicating that an increase in the value of the independent variable leads to an increase in the value of the dependent variable. Conversely, if $sgn(f) < 0$, the link has a negative polarity, indicating that an increase in the value of the independent variable leads to a decrease in the value of the dependent variable.

The following section provides a detailed account of the different iterations of the causal loop diagram (CLD) used in this study. Each version of the CLD is described in terms of its main assumptions, objectives, and causal relationships between variables. Additionally, we highlight the changes made from the previous version and provide a rationale for these modifications. By documenting the evolution of the CLD, we hope to provide readers with a better understanding of the modeling process and the insights gained through each iteration. Note that boxes represent state variables while other names are intermediate variables. A positive directed link (X → Y) means, *ceteris paribus*, increase (decrease) in X increases (decreases) Y above (below) what it would have been otherwise.

Version 1: Initial CLD
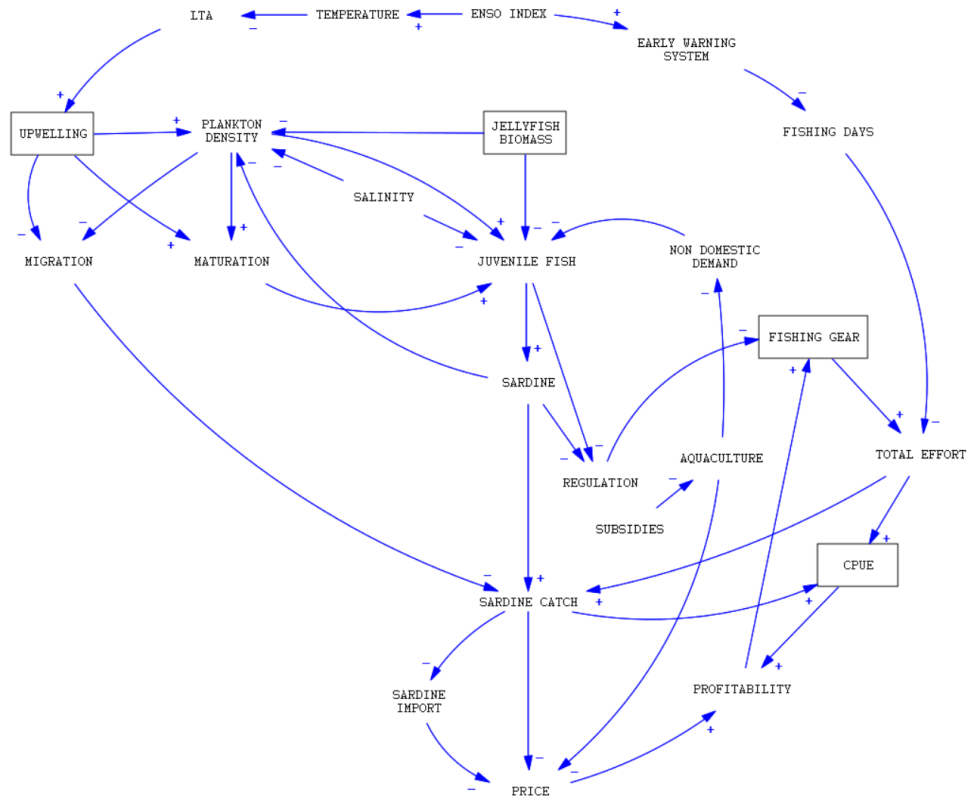
Figure A.1: This version of the causal loop diagram (CLD) shown in the figure reveals several notable omissions in the causal relationships between variables. Specifically, several causal links were missing, resulting in an incomplete representation of the system's dynamics. Additionally, the Jellyfish population, represented by the Jellyfish biomass variable, was considered a state variable. However, since it was not involved in any feedback loops, its inclusion in the model would not provide meaningful insights into the system's behaviour.

Version 2: Revised CLD
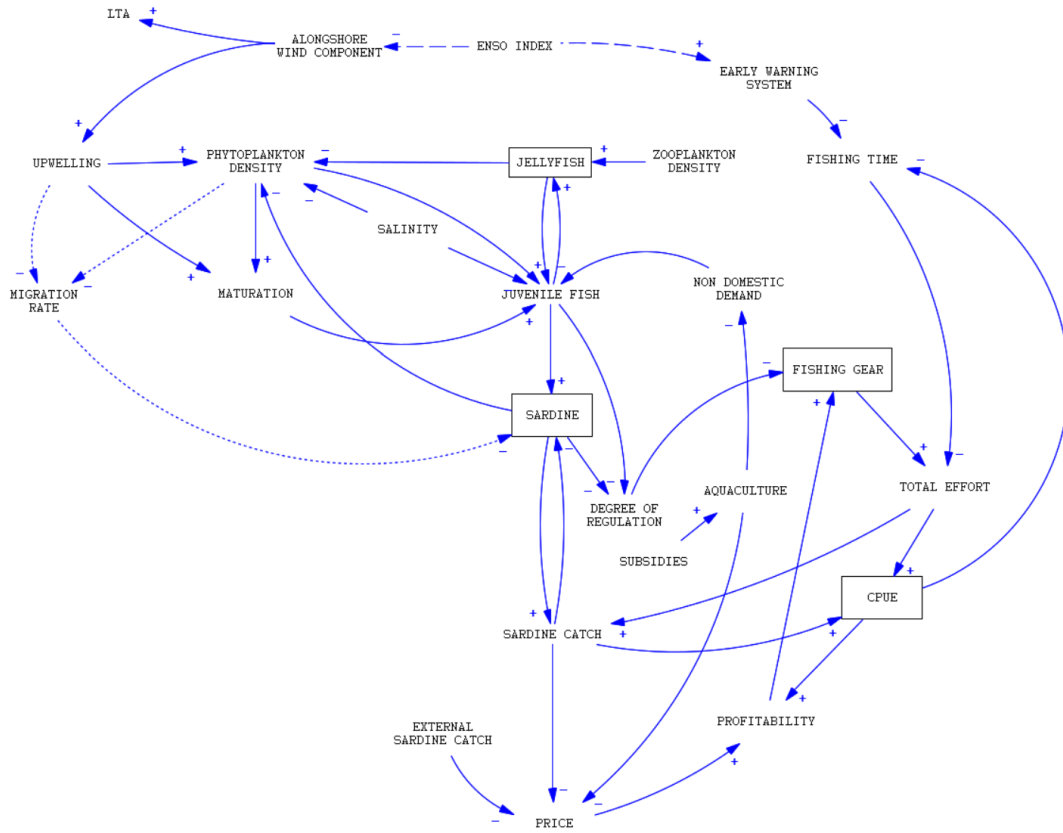
Figure A.2: This particular version of the causal loop diagram (CLD) shown in the figure underwent several significant updates and refinements. Notably, the causal links pertaining to upwelling were updated to reflect the fact that the local thermal anomaly (LTA) is an indicator of upwelling, rather than a direct cause. As part of this update, the Sardine population was also added as a state variable, while upwelling was redefined as an intermediate variable in the model. *Sardine import* was replaced by *External sardine catch*, which was added as a driver. To better capture the complex interconnections between different variables, dashed lines were introduced to represent teleconnections, while dotted lines were included to indicate potential model experiments. Additionally, several missing links were identified and subsequently added to improve the completeness and accuracy of the model.

Version 3: Updated CLD
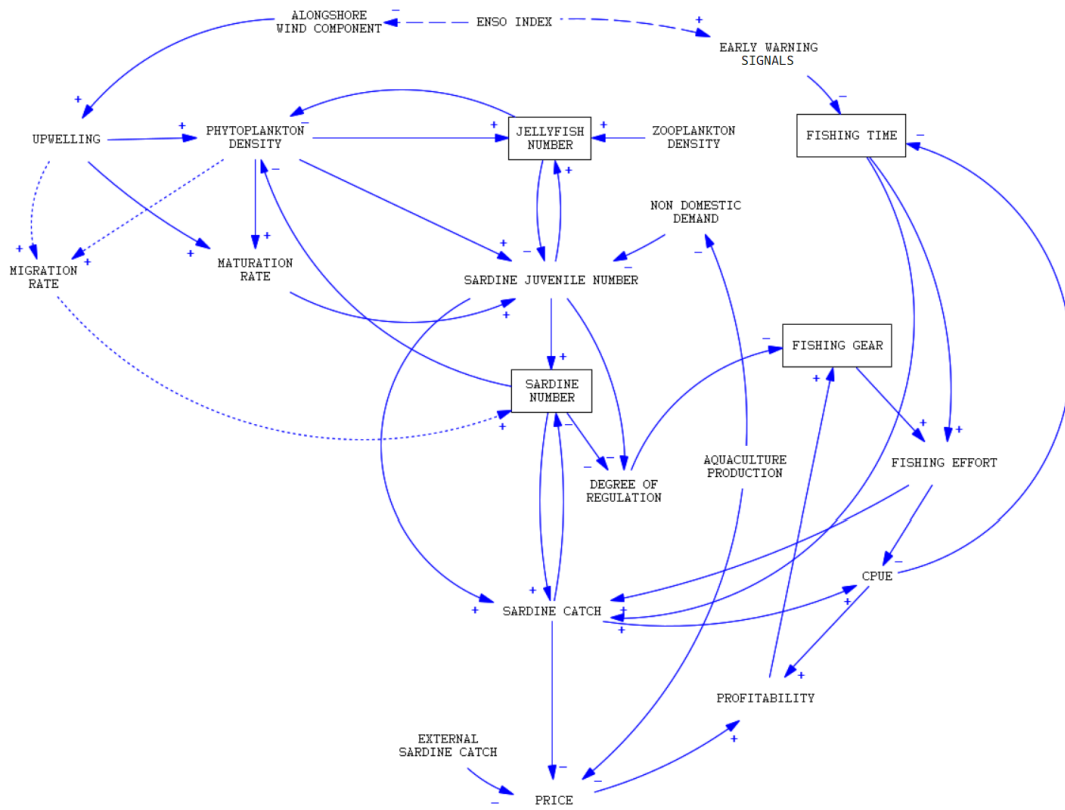
Figure A.3: The updated iteration of the causal loop diagram (CLD) shown in the figure underwent several key changes to improve its accuracy and stability. One notable update involved the replacement of the state variable CPUE with Fishing time, as the previous dynamical equation describing CPUE resulted in unstable fixed points due to a lack of a balancing term to prevent infinite growth (positive reinforcement). Instead, Fishing time was modeled using a delay equation to provide a more stable and realistic representation of the system's dynamics. Additionally, several missing links were identified and added to the model based on the system of equations, helping to improve the completeness and accuracy of the model. To reduce the complexity of the CLD, redundancies such as salinity and subsidies were removed. These updates and refinements were critical in producing a robust and reliable model that accurately captures the underlying causal relationships and dynamics of the system.
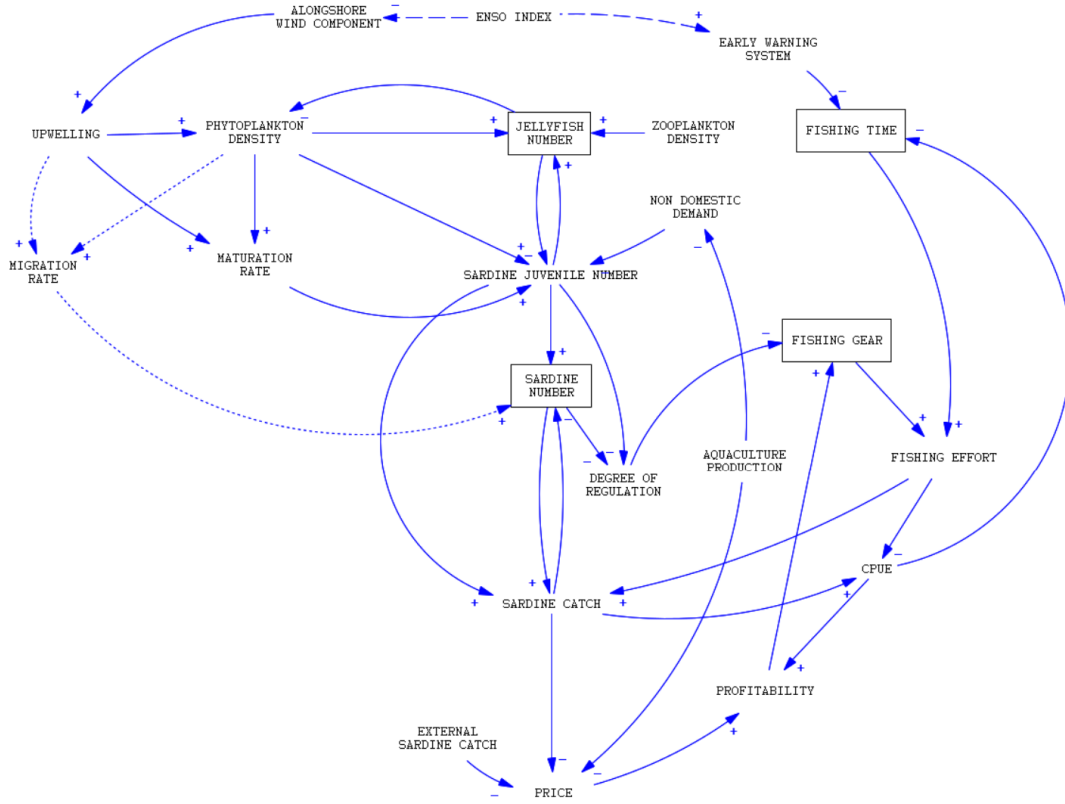
Figure A.4: The final version of the causal loop diagram (CLD) shown in the figure contains one key change that was identified while assessing the intermediate variable relationship of phytoplankton density(PHY) with sardine number(SN). The parameter $\eta[MN, SN]$ had very high sensitivity and variance ($\mu = 2.05355$, $\mu^* = 2.05760$, $\sigma = 1.2460$). OAT response curve revealed an unstable region between 0.4 and 1 for the baseline case. Note that migration number(MN) and sardine number(SN) are related through the intermediate variable equation $\eta[MN, SN] = \eta[MN, PHY] \cdot \eta[PHY, SN]$. Upon further examination of the feedback loop $SN > PHY > JFN > SJN > SN$, which is a reinforcing loop, it was found that $\eta[PHY, SN]$ needs to remain very small for the system to be stable (see Version 3). As a result, the redundant link was removed. This decision was justified by the fact that sardine number has a relatively small effect on phytoplankton density compared to environmental variables (Rai and Rajashekhar, 2014). Another redundant link from fishing time(FT) to sardine catch(SC) was also removed in this version.

A.2   Feedback loops in the system

Important feedback loops in the system are given below

Loop Number 1 of length 1
SARDINE JUVENILE NUMBER JELLYFISH NUMBER
Loop Number 2 of length 2
SARDINE JUVENILE NUMBER JELLYFISH NUMBER PHYTOPLANKTON DENSITY
Loop Number 3 of length 2
SARDINE JUVENILE NUMBER SARDINE NUMBER PHYTOPLANKTON DENSITY
Loop Number 4 of length 3
SARDINE JUVENILE NUMBER SARDINE NUMBER PHYTOPLANKTON DENSITY
JELLYFISH NUMBER
Loop Number 5 of length 3
SARDINE JUVENILE NUMBER SARDINE NUMBER PHYTOPLANKTON DENSITY
MATURATION RATE
Loop Number 6 of length 3
SARDINE JUVENILE NUMBER JELLYFISH NUMBER PHYTOPLANKTON DENSITY
MATURATION RATE
Loop Number 7 of length 3
SARDINE JUVENILE NUMBER SARDINE CATCH SARDINE NUMBER PHYTOPLANK-
TON DENSITY
Loop Number 8 of length 4
SARDINE JUVENILE NUMBER SARDINE CATCH SARDINE NUMBER PHYTOPLANK-
TON DENSITY MATURATION RATE
Loop Number 9 of length 4
SARDINE JUVENILE NUMBER SARDINE CATCH SARDINE NUMBER PHYTOPLANK-
TON DENSITY JELLYFISH NUMBER
Loop Number 10 of length 6
SARDINE JUVENILE NUMBER DEGREE OF REGULATION FISHING GEAR FISH-
ING EFFORT SARDINE CATCH SARDINE NUMBER PHYTOPLANKTON DENSITY
Loop Number 11 of length 7
SARDINE JUVENILE NUMBER DEGREE OF REGULATION FISHING GEAR FISH-
ING EFFORT SARDINE CATCH SARDINE NUMBER PHYTOPLANKTON DENSITY

MATURATION RATE

Loop Number 12 of length 7

SARDINE JUVENILE NUMBER DEGREE OF REGULATION FISHING GEAR FISHING EFFORT SARDINE CATCH SARDINE NUMBER PHYTOPLANKTON DENSITY JELLYFISH NUMBER

Loop Number 13 of length 8

SARDINE JUVENILE NUMBER DEGREE OF REGULATION FISHING GEAR FISHING EFFORT CPUE FISHING TIME SARDINE CATCH SARDINE NUMBER PHYTOPLANKTON DENSITY

Loop Number 14 of length 9

SARDINE JUVENILE NUMBER DEGREE OF REGULATION FISHING GEAR FISHING EFFORT CPUE FISHING TIME SARDINE CATCH SARDINE NUMBER PHYTOPLANKTON DENSITY MATURATION RATE

Loop Number 15 of length 9

SARDINE JUVENILE NUMBER DEGREE OF REGULATION FISHING GEAR FISHING EFFORT CPUE FISHING TIME SARDINE CATCH SARDINE NUMBER PHYTOPLANKTON DENSITY JELLYFISH NUMBER

A.3 Estimation of parameters used for calibrating the baseline mode

Alpha (α) parameters

Name	Definition	Range of value during regime shift (2010-2015)	References & Additional Comments
Sardine Number	$\frac{SardineMoralityNumber}{SardineNumber}$	1.34-2.7	(Rohit et al., 2018) (Nair et al., 2016)
Jellyfish Number	$\frac{JellyfishSenescentMortality}{JellyfishNumber}$	0.1	(Henschke et al., 2018)
Fishing Gear	Proportion of Gear Loss for Ring Seine Gears	0.292-0.368	(Daniel and Thomas, 2022) Total Mean ± S.D of ALDFG for both large and small RS gears divided by total used gear (in kg.vessel−1 year−1)
Fishing Time	$\frac{FishingTime}{FishingTime}$	1	By definition

Beta (β) parameters

Name	Definition	Range of value during regime shift (2010-2015)	References & Additional Comments
Sardine Recruitment	Proportional increase in sardine number due to recruitment	$Uniform(0,1)$	uniform distribution assumed
Sardine Natural Mortality	$\frac{NaturalMortality}{TotalMortality}$	0.2	(Rohit et al., 2018) (page 74). Data available is along the Indian coast during 2010-2015.
Sardine Catch	$\frac{FishingMortality}{TotalMortality}$	0.8	same as above.
Jellyfish Growth	Proportional increase in Jellyfish number due to gamogenesis	$Uniform(0,1)$	(Henschke et al., 2018) uniform distribution assumed.
Jellyfish Strobilation	Proportional increase in Jellyfish number due to medusa strobilation	$Uniform(0,1)$	(Henschke et al., 2018) uniform distribution assumed.
Jellyfish Predation Mortality	Proportion of decrease in Jellyfish number due to predation	0.85	(Henschke et al., 2018) for scaling coefficient, and (Kripa et al., 2018) for Jellyfish data from Kerala. Density-dependent predation function from the former paper was used for calculation.

Name	Definition	Range of value during regime shift (2010-2015)	References & Additional Comments
Jellyfish senescence	Proportion of decrease in Jellyfish number due to starvation/senescence	0.15	Model from above paper ((Henschke et al., 2018)) was used.
Fishing Gear (OBRS)	Proportion of OBRS gear	0.61-0.676	(Abdussamad et al., 2015) (Time series data available)
Fishing Gear (IBRS)	Proportion of IBRS gear	0324-0.381	(Abdussamad et al., 2015) (Time series data available)
Fishing compensated time	Proportional decrease in fishing time due to increase in CPUE	0.92-0.96	Fishers tend to satisfice even though it is technically possible to maximise profit by increasing effort. This could be due to social, economic or cultural reasons.
Fishing time loss	Proportional decrease in fishing time due to extreme events	0.04-0.08	(Martin et al., 2022)

Elasticities (η)

Function F_j	Variable X_i	Range of value during regime shift (2010-2015)	References & Additional Comments
Sardine Natural Mortality	Sardine Number	1	Linear mortality assumption.
Sardine Catch	Fishing Gear	$Uniform(0,1)$	(Kripa et al., 2018)
Sardin Recruitment	Jellyfish Number	$Uniform(0,1)$	(Kripa et al., 2018)
Sardine Catch	Jellyfish Number	$Uniform(0,1)$	(Kripa et al., 2018)
Migration Number	Jellyfish Number	$Uniform(0,1)$	(Benoit-Bird and Moline, 2021) Pelagic fishes may engage in vertical migration, with fish moving to deeper depths during the day to avoid predators and returning to the surface at night to feed. However, some pelagic fish species may also exhibit longer-term vertical migrations.
Sardine Recruitment	Sardine Number	1	Approximate flow into adult age group proportional to juvenile number.

Function F_j	Variable X_i	Range of value during regime shift (2010-2015)	References & Additional Comments
Sardine Catch	Sardine Number	0.64-0.75	(Harley et al., 2001) (Erisman et al., 2011)
Sardine Natural Mortality	Jellyfish Number	$Uniform(0,1)$	(Kripa et al., 2018)
Jellyfish Growth	Sardine Number	$Uniform(0,1)$	(Kripa et al., 2018)
Jellyfish Strobilation	Jellyfish Number	$Uniform(0,1)$	(Henschke et al., 2018)
Jellyfish Predation Mortality	Jellyfish Number	$Uniform(0.5,1.5)$	(Henschke et al., 2018)
Jellyfish Senescence	Jellyfish number	1	(Henschke et al., 2018) Linearly proportional to Medusa number.
Gear Exit	Fishing Gear	1	Linear exit/loss assumption.
Sardine Catch	Fishing Time	$Uniform(0.5,1)$	(Lade et al., 2015)
Fishing Gear (OBRS)	Fishing Time	$Uniform(0,1)$	
Fishing Gear (IBRS)	Fishing Time	$Uniform(0,1)$	
Gear Exit	Fishing Time	$Uniform(0,1)$	
Fishing Compensated Time	Fishing Time	1	Linear compensation assumption
Loss in Fishing Time	Fishing Time	$Uniform(0,1)$	

Function F_j	Variable X_i	Range of value during regime shift (2010-2015)	References & Additional Comments
Fishing Compensated Time	Fishing Gear	$Uniform(0,1)$	
Fishing Time	Fishing Gear	$Uniform(0,1)$	
Fishing Time	Sardine Number	$Uniform(0,0.75)$	We chose the upper bound to be same as that of η(Sardine Catch, Sardine Number)
Fishing Compensated Time	Sardine Number	$Uniform(0,0.75)$	same as above

Parameter	Value
a_SN	1.34
a_JFN	0.1
a_FG	0.33
a_FT	1

(a) Alpha (α) parameters

Parameter	Value
b_SRIA	0.5*
b_MN	0.5*
b_SC	0.8
b_SMN	0.2
b_JFG	0.3*
b_JFMS	0.7*
b_JFPM	0.85
b_JFS	0.15
b_FGOBRS	0.62
b_FGIBRS	0.38
b_FCT	0.8*
b_LFT	0.2*

(b) Beta (β) parameters

Parameter	Value
EE_SRIA_SN	1 †
EE_SC_SN	0.6*
EE_SMN_SN	1 †
EE_SRIA_JFN	0.75*
EE_MN_JFN	0.6*
EE_SC_JFN	0.3*
EE_SMN_JFN	0.8*
EE_SC_FG	0.8*
EE_JFG_SN	0.6*
EE_JFMS_JFN	0.8*
EE_JFPM_JFN	1 †
EE_JFS_JFN	1 †
EE_FGOBRS_SN	0.3*
EE_FGIBRS_SN	0.4*
EE_GE_SN	0.35*
EE_FGOBRS_FG	1 †
EE_FGIBRS_FG	0.8*
EE_GE_FG	1 †
EE_SC_FT	0.5*
EE_FGOBRS_FT	0.3*
EE_FGIBRS_FT	0.4*
EE_GE_FT	0.2*
EE_FCT_FT	0.6*
EE_LFT_FT	0.5*
EE_FCT_FG	0.6*
EE_FT_FG	0.1*
EE_FT_SN	0.1*
EE_FCT_SN	0.6*

(c) Elasticities (η)

Table A.1: Baseline parameters used for the OAT sensitivity analysis

† A linear relationship is assumed.

* This analysis employed ad-hoc values denoted by an asterisk to represent parameters that were not derived from empirical data. The selection of these values was based on heuristics, specifically to prioritize balancing feedback loops over reinforcing feedback loops. The optimization was then implemented to achieve convergence towards a stable fixed point.

A.4   Morris Sensitivity Analysis

Morris sensitivity analysis (Morris, 1991) is a global sensitivity analysis method used to measure the effect of the input variables on the output of a model. It is based on the concept of elementary effects, which are the changes in the model output caused by varying one input variable while keeping the others constant.

The elementary effect of a single input variable is defined as:

$$\delta_i = \frac{f(\mathbf{x} + e_i \Delta) - f(\mathbf{x})}{\Delta}$$

where δ_i is the ith elementary effect for a model with k independent inputs discretized into a p-level grid Ω, $f(\mathbf{x})$ is the model output when the ith input variable is set to a selected value $\mathbf{x}_i \in \Omega$, $f(\mathbf{x} + e_i \Delta)$ is the transformed model output when all input variables except the ith are set to their original values, e_i is a vector of zeros but with a unit as its ith component, and Δ is a value in $\{\frac{1}{p-1}, ..., 1 - \frac{1}{p-1}\}$.

To calculate the global sensitivity indices using the Morris method, the elementary effects are first sorted according to their absolute values. The sorted effects are then grouped into bins, and the mean absolute effect and standard deviation of the absolute effect are calculated for each bin. The global sensitivity indices, μ_i and σ_i, are then calculated as:

$$\mu_i = \frac{1}{N} \sum_{k=1}^{N} \delta_i^{(k)}, \quad \sigma_i = \sqrt{\frac{1}{N-1} \sum_{k=1}^{N} (\delta_i^{(k)} - \mu_i)^2}$$

where N is the total number of evaluations. The μ_i value is a measure of the average effect of the ith input variable on the model output, while the σ_i value is a measure of the variability of the effect across different evaluations. Together, μ_i and σ_i provide a measure of the

importance of the ith input variable in the model. To take into account of both positive and negative effects when the distribution of input variable is non-uniform, a modified index was proposed (Campolongo et al., 2007) replacing the use of the mean with μ^*, which is defined as the estimate of the mean of the distribution of the absolute values of the elementary effects.

To perform Morris sensitivity analysis with SALib, you must first define your model input parameters and ranges. Then you need to run the model multiple times using different parameter combinations generated by the SALib library. Finally, the sensitivity indices can be calculated based on the output generated by the model runs. The sensitivity indices give you an idea of which input parameters are most important in influencing the model output.

A.5 Worked-out Example

To deepen our understanding of the methodology, we examined an ecological model as an illustrative example. We used a three-dimensional age-structured prey-predator (APP) model (Negahbani et al., 2016) with exact equations to study the stability of the system and the sensitivity of the parameters. The model describes interaction dynamics between a predator and an age-structured prey composed of juvenile and adult developmental stages. The scaled model equations are as follows:

$$
\begin{aligned}
\frac{dJ}{dt} = f_1(J, A, P) &= bA - \frac{J}{1 + J^2} - \mu_J J \\
\frac{dA}{dt} = f_2(J, A, P) &= \frac{J}{1 + J^2} - AP - \mu_A A \\
\frac{dP}{dt} = f_3(J, A, P) &= cAP - \mu_P P
\end{aligned}
\tag{A.1}
$$

where J, A, and P are state variables describing the size of juvenile, adult and prey populations respectively. Here b is the reproduction rate of adults, and c is the predator conversion efficiency. Death rates are μ_J, μ_A, and μ_P for juvenile, adult and predator populations, respectively.

Using (2.7), the jacobian matrix for the model in terms of generalized parameters is as follows:

$\alpha_J \cdot (-\beta_{f_{12}} \cdot \eta[f_{12}, J] - (1 - \beta_{f_{12}}))/(1 - \beta_{f_{12}})$	$\alpha_J/(1 - \beta_{f_{12}})$	0
$\alpha_A \cdot \eta[f_{12}, J]/\beta_{f_{23}}$	$-\alpha_A/\beta_{f_{23}}$	$\alpha_A \cdot (\beta_{f_{23}} - 1)/\beta_{f_{23}}$
0	α_P	0

Here, we have used death rates as the respective alpha parameters for the state variables $J, A,$ and P.

Parameter	Value
α_J	0.05
α_A	0.1
α_P	[0, 0.43525]
$\beta_{f_{12}}$	[0.8, 0.952]
$\beta_{f_{23}}$	[0.1, 0.111]
$\eta[f_{12}, J]$	[0, 0.6]

Table A.2: **Generalized parameters (APP model).** We assigned values for generalized parameters using the same values as in the original model. However, we limited the range of α_P to the stable region until the saddle-node bifurcation at the left-hand turning point. The function f_{ij} corresponds to a process in the model equation, following the same order as given in the paper.
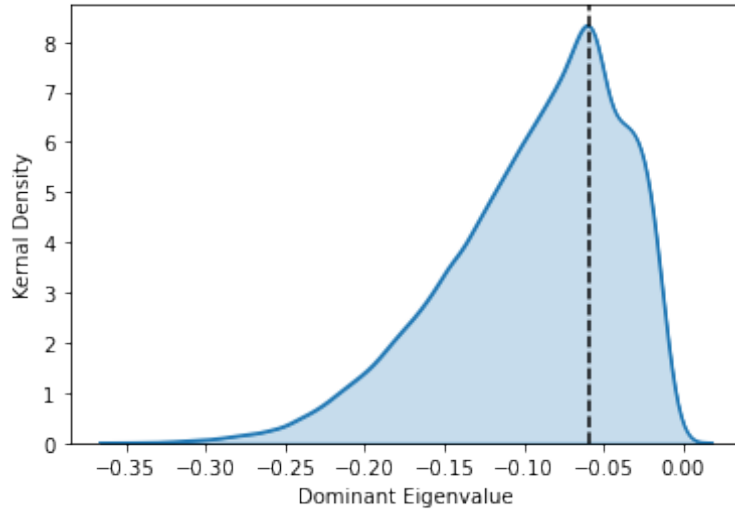
Figure A.5: **Distribution of instability (APP model).** Kernal density of distribution of dominant eigenvalues for the APP model estimated from a Latin hypercube sampling simulation (positive/negative numbers indicate an unstable/stable system). The maximum distribution density is at eigenvalue = -0.05929. The sampled points are from the unstable region since we chose the parameter region accordingly.
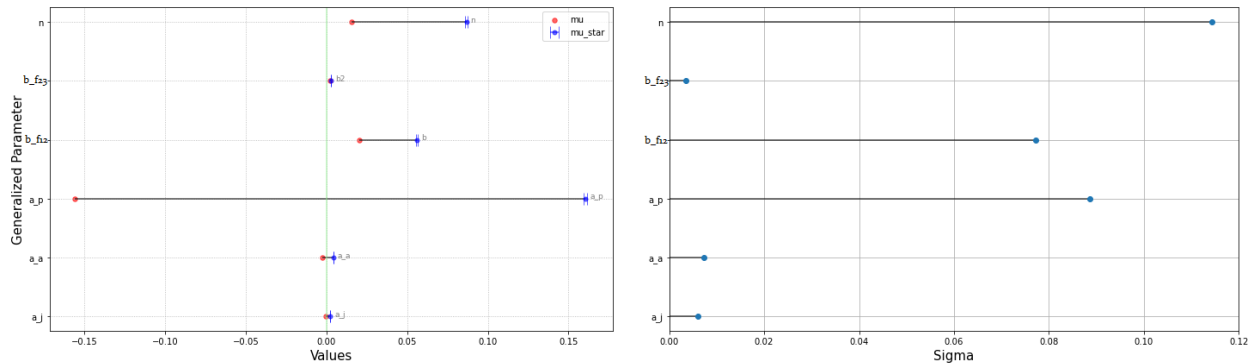

Figure A.6: **Morris Sensitivity Analysis (APP model).** (a) Sensitivity values of the parameters against the real part of the dominant eigenvalue. The stability of the model is most sensitive to α_P (death rate of the predator), and it has a stabilizing effect ($\mu = -0.1556$, $\sigma = 0.08857$). (b) The uncertainty (σ) associated with each parameter is shown. The parameters $\eta, \beta_{f_{12}}, \alpha_P$ have relatively higher uncertainty since their sensitivity depends on the choice of other parameters as well.

Bibliography

Abdussamad, E., Ganga, U., Koya, K., Prakasan, D., and Gireesh, R. (2015). Ring seine fishery of kerala: An overview. *Marine Fisheries Information Service; Technical and Extension Series*, (225):3–7.

Achuthavarier, D., Krishnamurthy, V., Kirtman, B. P., and Huang, B. (2012). Role of the indian ocean in the enso–indian summer monsoon teleconnection in the ncep climate forecast system. *Journal of climate*, 25(7):2490–2508.

Annigeri, G. (1971). Estimation of mortality rates of the oil sardine, sardinella longiceps val. *Indian Journal of Fisheries*, 18(1&2):109–113.

Ashwin, P., Wieczorek, S., Vitolo, R., and Cox, P. (2012). Tipping points in open systems: bifurcation, noise-induced and rate-dependent examples in the climate system. *Philosophical Transactions of the Royal Society A: Mathematical, Physical and Engineering Sciences*, 370(1962):1166–1184.

Baudin, M., Christopoulou, M., Colette, Y., and Martinez, J. (2013). pydoe: The experimental design package for python.

Benoit-Bird, K. J. and Moline, M. A. (2021). Vertical migration timing illuminates the importance of visual and nonvisual predation pressure in the mesopelagic zone. *Limnology and Oceanography*, 66(8):3010–3019.

Biggs, R., De Vos, A., Preiser, R., Clements, H., Maciejewski, K., and Schlüter, M. (2021). *The Routledge handbook of research methods for social-ecological systems*. Taylor & Francis.

Campolongo, F., Cariboni, J., and Saltelli, A. (2007). An effective screening design for sensitivity analysis of large models. *Environmental modelling & software*, 22(10):1509–1518.

CMFRI, K. (2007). Cmfri newsletter no. 115 july-september 2007.

Daniel, D. B. and Thomas, S. N. (2022). Abandoned, lost and discarded fishing gear from the fishing sector of kerala, india. *Ocean Science Journal*, pages 1–13.

Erisman, B. E., Allen, L. G., Claisse, J. T., Pondella, D. J., Miller, E. F., and Murray, J. H. (2011). The illusion of plenty: hyperstability masks collapses in two recreational fisheries that target fish spawning aggregations. *Canadian Journal of Fisheries and Aquatic Sciences*, 68(10):1705–1716.

Gross, T. (2004). *Population dynamics: General results from local analysis*. PhD thesis, Universität Oldenburg.

Gross, T., Ebenhöh, W., and Feudel, U. (2005). Long food chains are in general chaotic. *Oikos*, 109(1):135–144.

Gross, T. and Feudel, U. (2006). Generalized models as a universal approach to the analysis of nonlinear dynamical systems. *Physical Review E*, 73(1):016205.

Harley, S. J., Myers, R. A., and Dunn, A. (2001). Is catch-per-unit-effort proportional to abundance? *Canadian Journal of Fisheries and Aquatic Sciences*, 58(9):1760–1772.

Henschke, N., Stock, C. A., and Sarmiento, J. L. (2018). Modeling population dynamics of scyphozoan jellyfish (aurelia spp.) in the gulf of mexico. *Marine Ecology Progress Series*, 591:167–183.

Herman, J. and Usher, W. (2017). SALib: An open-source python library for sensitivity analysis. *The Journal of Open Source Software*, 2(9).

Holmes, P. and Shea-Brown, E. T. (2006). Stability. *Scholarpedia*, 1(10):1838. revision #137538.

Iwanaga, T., Usher, W., and Herman, J. (2022). Toward SALib 2.0: Advancing the accessibility and interpretability of global sensitivity analyses. *Socio-Environmental Systems Modelling*, 4:18155.

Jin, R., Chen, W., and Sudjianto, A. (2003). An efficient algorithm for constructing optimal design of computer experiments. In *International design engineering technical conferences and computers and information in engineering conference*, volume 37009, pages 545–554.

Kripa, V., Mohamed, K. S., Koya, K. S., Jeyabaskaran, R., Prema, D., Padua, S., Kuriakose, S., Anilkumar, P., Nair, P. G., Ambrose, T., et al. (2018). Overfishing and climate drives changes in biology and recruitment of the indian oil sardine sardinella longiceps in southeastern arabian sea. *Frontiers in Marine Science*, 5:443.

Kuehn, C. (2011). A mathematical framework for critical transitions: Bifurcations, fast–slow systems and stochastic dynamics. *Physica D: Nonlinear Phenomena*, 240(12):1020–1035.

Kuehn, C., Siegmund, S., and Gross, T. (2013). Dynamical analysis of evolution equations in generalized models. *The IMA Journal of Applied Mathematics*, 78(5):1051–1077.

Lade, S. J. and Gross, T. (2012). Early warning signals for critical transitions: a generalized modeling approach. *PLoS computational biology*, 8(2):e1002360.

Lade, S. J. and Niiranen, S. (2017). Generalized modeling of empirical social-ecological systems. *Natural Resource Modeling*, 30(3):e12129.

Lade, S. J., Niiranen, S., Hentati-Sundberg, J., Blenckner, T., Boonstra, W. J., Orach, K., Quaas, M. F., Österblom, H., and Schlüter, M. (2015). An empirical model of the baltic sea reveals the importance of social dynamics for ecological regime shifts. *Proceedings of the National Academy of Sciences*, 112(35):11120–11125.

Longhurst, A. R. and Wooster, W. S. (1990). Abundance of oil sardine (sardinella longiceps) and upwelling on the southwest coast of india. *Canadian Journal of Fisheries and Aquatic Sciences*, 47(12):2407–2419.

Lotka, A. J. (1925). *Elements of physical biology*. Williams & Wilkins.

Lynam, C. P., Hay, S. J., and Brierley, A. S. (2005). Jellyfish abundance and climatic variation: contrasting responses in oceanographically distinct regions of the north sea, and possible implications for fisheries. *Journal of the Marine Biological Association of the United Kingdom*, 85(3):435–450.

Martin, M., Abhilash, S., Pattathil, V., Harikumar, R., Niyas, N., Nair, T. B., Grover, Y., and Osella, F. (2022). Should i stay or should i go? south indian artisanal fishers' precarious livelihoods and their engagement with categorical ocean forecasts. *Weather, Climate, and Society*, 14(1):113–129.

Massing, J. C. and Gross, T. (2021). Generalized modeling: A survey and guide. *arXiv preprint arXiv:2112.00360*.

Mohamed, K., Zacharia, P., Maheswarudu, G., Sathianandan, T., Abdussamad, E., Ganga, U., Pillai, S. L., Sobhana, K., Nair, R. J., Josileen, J., et al. (2014). Minimum legal size (mls) of capture to avoid growth overfishing of commercially exploited fish and shellfish species of kerala. *Marine Fisheries Information Service; Technical and Extension Series*, (220):3–7.

Morris, M. D. (1991). Factorial sampling plans for preliminary computational experiments. *Technometrics*, 33(2):161–174.

Muni Krishna, K. (2008). Coastal upwelling along the southwest coast of india–enso modulation. In *Annales Geophysicae*, volume 26, pages 1331–1334. Copernicus Publications Göttingen, Germany.

Nair, P. G., Joseph, S., Kripa, V., Remya, R., and Pillai, V. (2016). Growth and maturity of indian oil sardine sardinella longiceps (valenciennes, 1847) along southwest coast of india. *Journal of the Marine Biological Association of India*, 58(1):64–68.

Negahbani, E., Steyn-Ross, D. A., Steyn-Ross, M. L., and Aguirre, L. A. (2016). Which system variables carry robust early signs of upcoming phase transition? an ecological example. *PloS one*, 11(9):e0163003.

Nguyen, Q. and Leung, P. (2013). Revenue targeting in fisheries. *Environment and Development Economics*, 18(5):559–575.

Ott, E. (2006). Basin of attraction. *Scholarpedia*, 1(8):1701. revision #170495.

Quaas, M. F. and Requate, T. (2013). Sushi or fish fingers? seafood diversity, collapsing fish stocks, and multispecies fishery management. *The Scandinavian Journal of Economics*, 115(2):381–422.

Rai, S. V. and Rajashekhar, M. (2014). Seasonal assessment of hydrographic variables and phytoplankton community in the arabian sea waters of kerala, southwest coast of india. *Brazilian Journal of Oceanography*, 62:279–289.

Reyers, B., Folke, C., Moore, M.-L., Biggs, R., and Galaz, V. (2018). Social-ecological systems insights for navigating the dynamics of the anthropocene. *Annual Review of Environment and Resources*, 43:267–289.

Rohit, P., Sivadas, M., Abdussamad, E., Margaret Muthu Rathinam, A., Koya, K., Ganga, U., Ghosh, S., Rajesh, K., Mohammed Koya, K., Chellappan, A., et al. (2018). *Enigmatic Indian oil sardine: An insight.* Number 130. ICAR-Central Marine Fisheries Research Institute.

Saltelli, A. and Giampietro, M. (2015). The fallacy of evidence based policy. *arXiv preprint arXiv:1607.07398.*

Saltelli, A., Guimaraes Pereira, Â., Van der Sluijs, J. P., and Funtowicz, S. (2013). What do i make of your latinorum? sensitivity auditing of mathematical modelling. *International Journal of Foresight and Innovation Policy*, 9(2-3-4):213–234.

Shyam, S. S., Rahman, M. R., and Antony, B. (2015). Sardine economy of kerala: paradigms and perspectives. *International Journal of Fisheries and Aquatic Studies*, 2(6):351–356.

Simon, H. A. (1955). A behavioral model of rational choice. *The quarterly journal of economics*, pages 99–118.

Sterman, J. (2010). *Business dynamics.* Irwin/McGraw-Hill c2000..

Virtanen, P., Gommers, R., Oliphant, T. E., Haberland, M., Reddy, T., Cournapeau, D., Burovski, E., Peterson, P., Weckesser, W., Bright, J., van der Walt, S. J., Brett, M., Wilson, J., Millman, K. J., Mayorov, N., Nelson, A. R. J., Jones, E., Kern, R., Larson, E., Carey, C. J., Polat, İ., Feng, Y., Moore, E. W., VanderPlas, J., Laxalde, D., Perktold, J., Cimrman, R., Henriksen, I., Quintero, E. A., Harris, C. R., Archibald, A. M., Ribeiro, A. H., Pedregosa, F., van Mulbregt, P., and SciPy 1.0 Contributors (2020). SciPy 1.0: Fundamental Algorithms for Scientific Computing in Python. *Nature Methods*, 17:261–272.

Yeakel, J. D., Stiefs, D., Novak, M., and Gross, T. (2011). Generalized modeling of ecological population dynamics. *Theoretical Ecology*, 4:179–194.